Sciences Chimiques de Rennes
UMR CNRS 6226

Bidimensional integration for powder diffraction

Carmelo PRESTIPINO

cnrs dépasser les frontières

UNIVERSITÉ DE RENNES 1 ueb

Outline of the talk

- Principle and comparison for bidimensional detector diffraction
- Main step during integration
- Hand on Tutorial with Fit2D

Preamble

- The use of two-dimensional detectors with synchrotron radiation enjoys a growing popularity.
- It is now possible to record the entire Debye - Scherrer rings at high angle and good resolution from few minutes to fractions of second.
- The field of applications is vast including texture analysis (Wenk & Grigull, 2003) and in situ powder diffraction measurements in dependence on pressure (Hanfland et al., 1999), temperature (Norby, 1997), chemical composition (Meneghini et al.,2001),

Meneghini et al,2001 Multipurpose imaging-plate camera for in situ powder XRD at the GILDA beamline. Journal of Synchrotron Radiation 8, 1162-1166.
Hanfland,M., (1999) Crystal structure of the high-pressure phase silicon VI. Physical Review Letters 82, 1197.
Norby, P. (1997) Synchrotron Powder Diffraction using Imaging Plates: Crystal Structure Determination and Rietveld Refinement. J App Crys 30, 21-30.

Chronology

First bidimensional detector for powder diffraction film is the film in Debye-Scherrer camera.

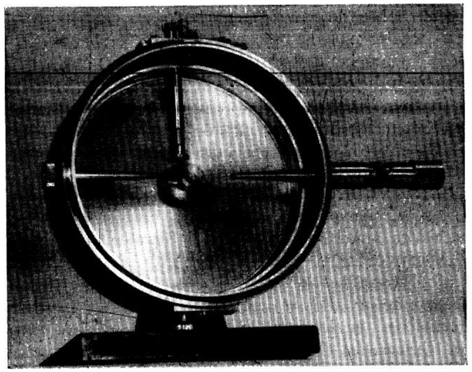

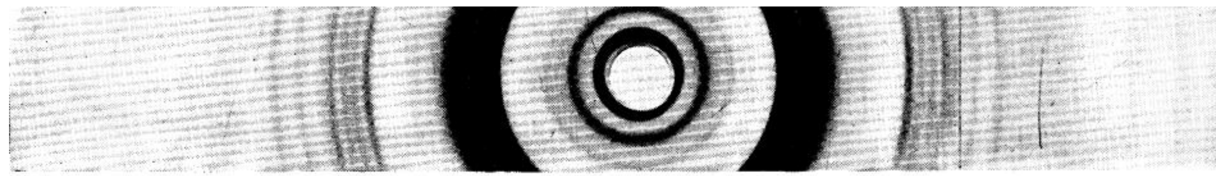

First experiments beginning of the nineties, only utilized thin equatorial strips (Norby, 1997).

Introduction of freely available software the integration of the entire image to a standard one-dimensional powder diffraction pattern (Hammersley et al., 1996)

Two-dimensional detector

Cylindrical

☺ High angular range

☹Fixed and ☺ constant spatial resolution

☹ Complicated and fixed experiment geometry

Maud could handle it!!!

Flat

☹ Size dependent angular range (limited)

☺ Variable spatial resolution distance sample detector

☺Easy experiment geometry

☺Cheaper (IP 70-100 k€)

Calibration & Integration

Extraction of standard powder diffractograms from two-dimensional images requires knowledge of the diffraction and azimuthal angle at each pixel.

Detector characteristics

- **The dynamic range** of the detector limits the intensity differences that are recordable on one image. The higher the dynamic range stronger is the available contrast. (bigger grey scale for your image)

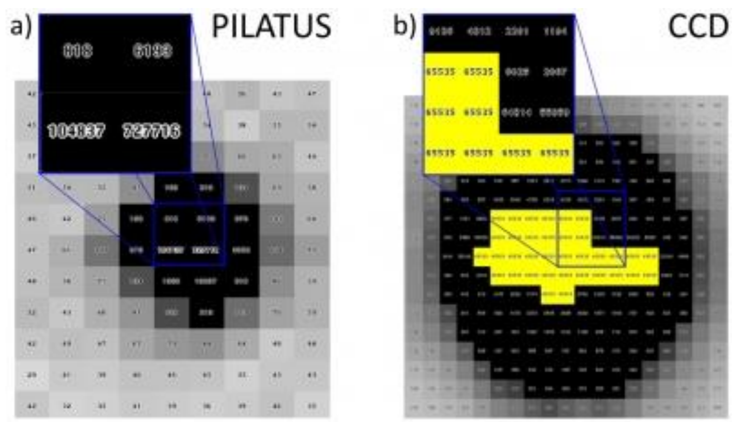

$$DQE = \frac{\left[\frac{I_{out}^2}{\sigma_{out}^2}\right]}{\left[\frac{I_{in}^2}{\sigma_{in}^2}\right]}$$

- **The detective quantum efficiency** (DQE) is a measure (to noise ratio reduction related to detector effectiveness.

Detector characteristics

- **Point spread function** (PSF) – the detectors signal to a delta function stimulus. Generally give the signal a Gaussian spread.

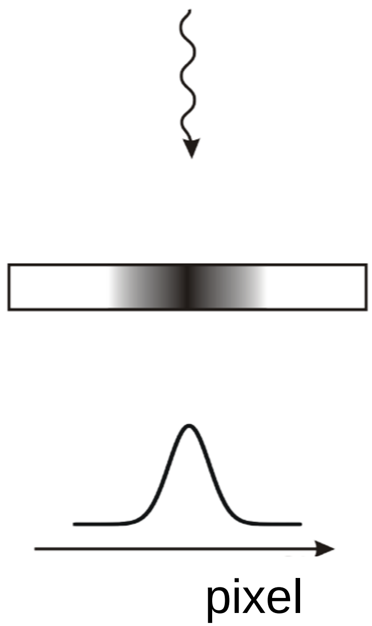

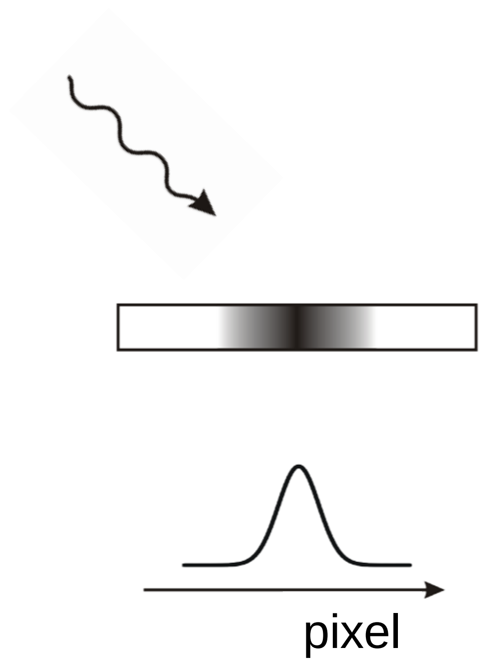

Basic ideal geometry

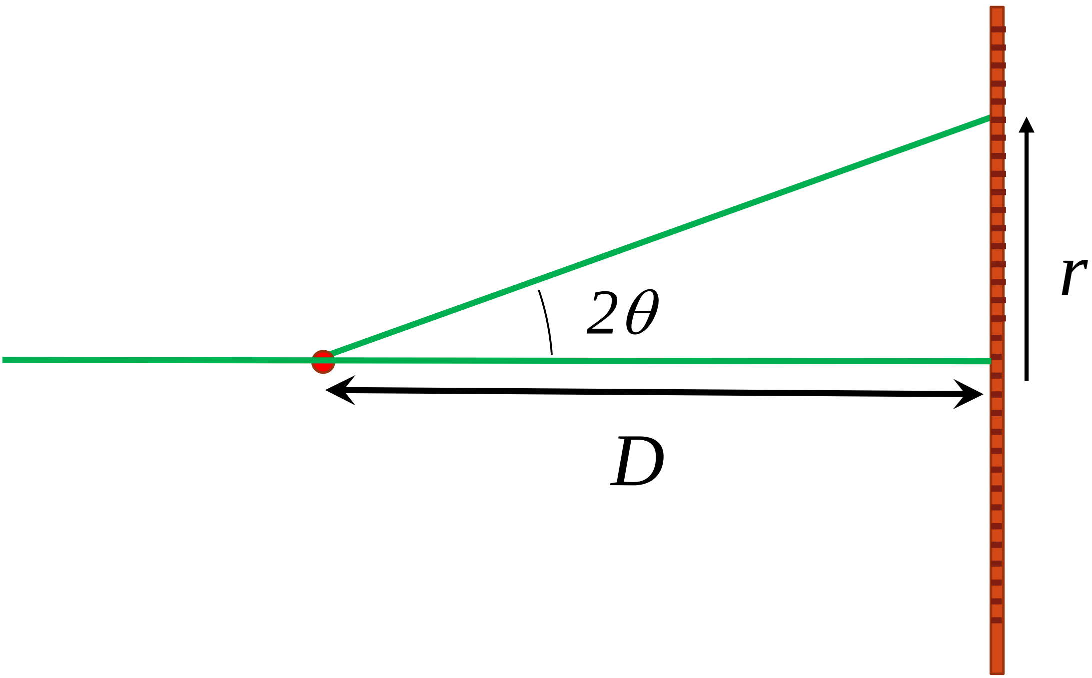

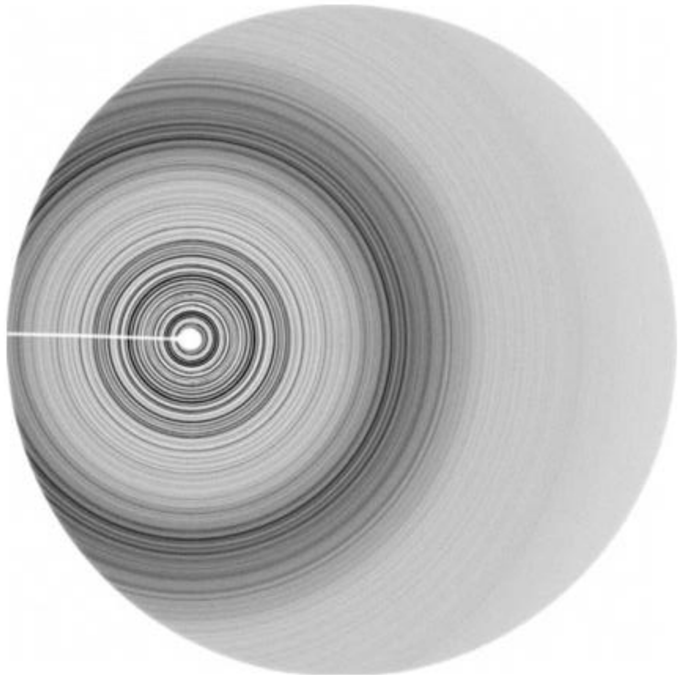

$$D \tan 2\theta = r$$

Basic ideal geometry

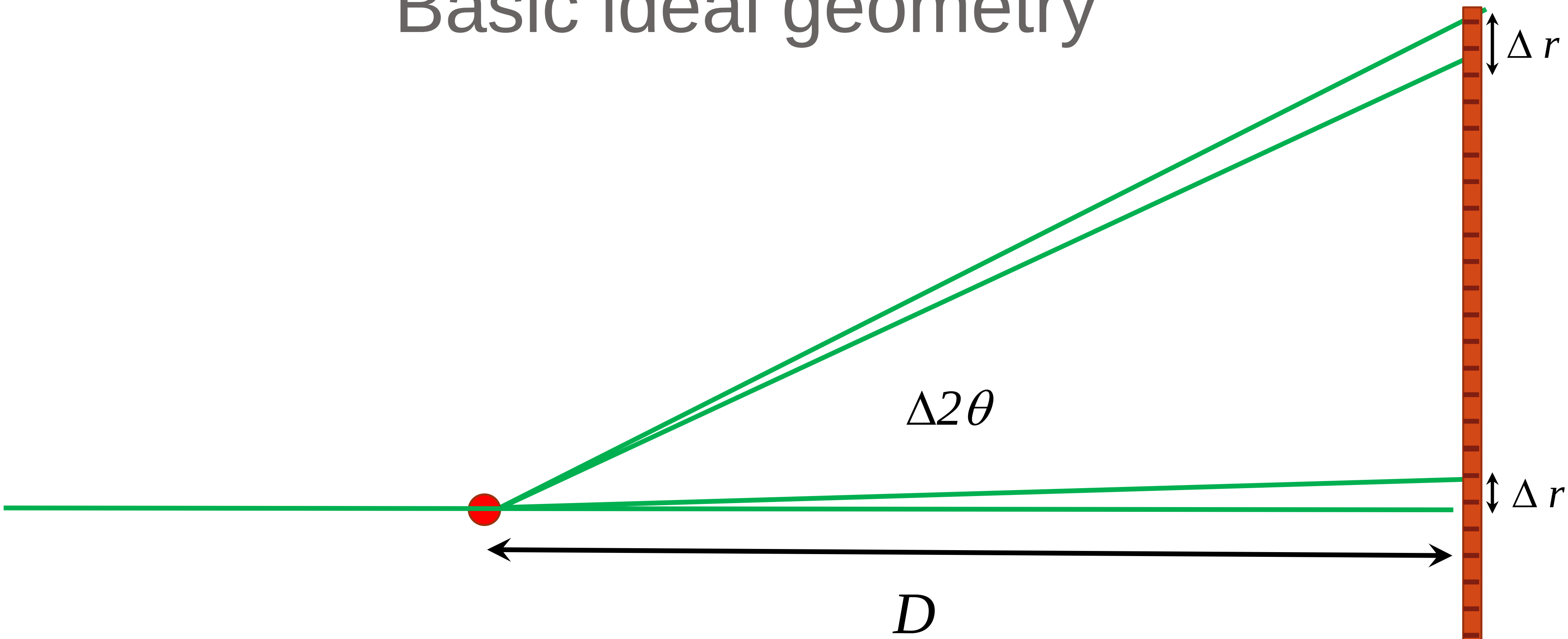

$$D \tan 2\theta = r$$

$$\frac{D}{\cos^2(2\theta)}\, d2\theta = dr$$

Basic ideal geometry
finite beam

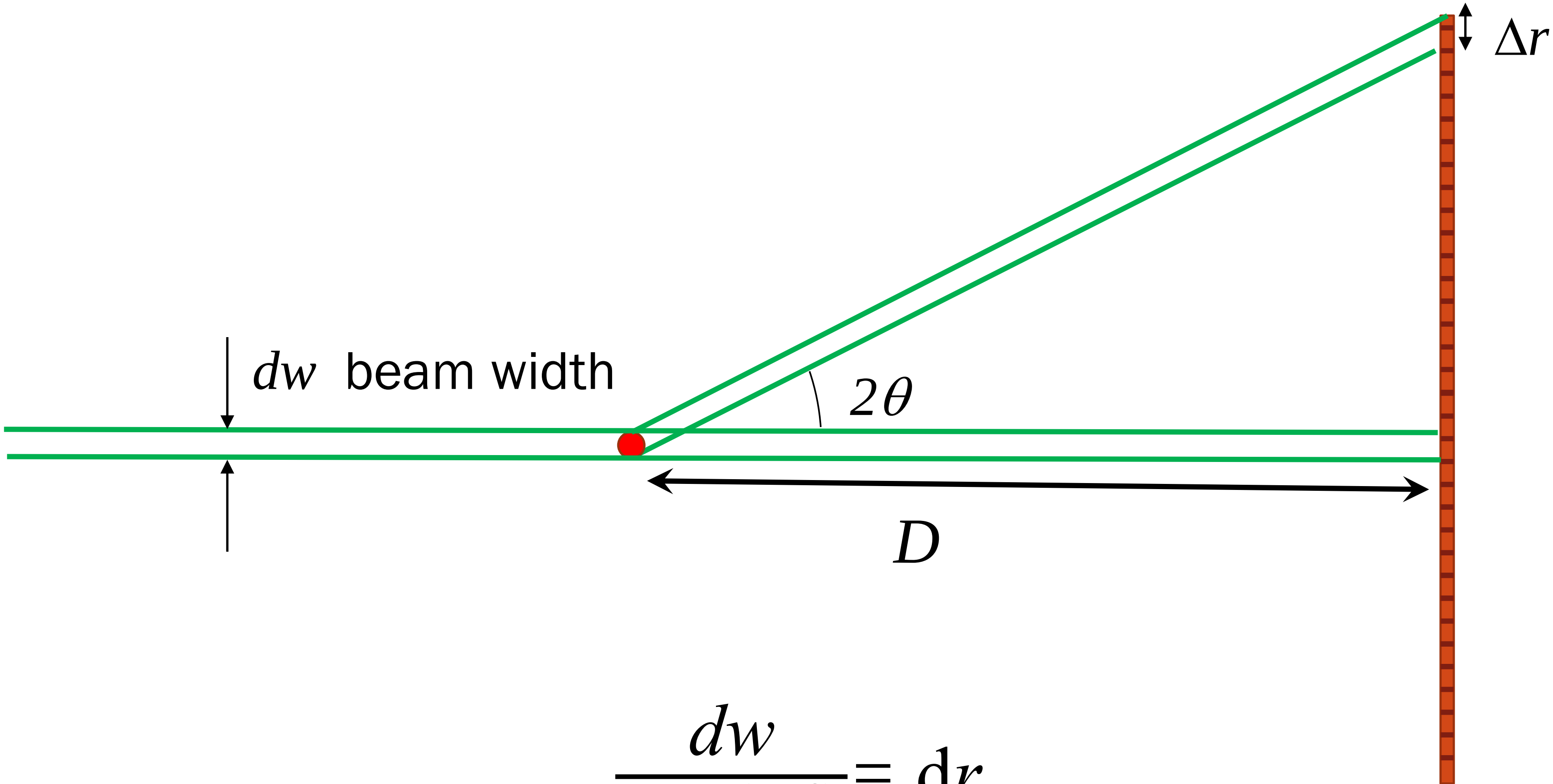

$$\frac{dw}{\cos(2\theta)} = \mathrm{d}r$$

Basic ideal geometry
finite beam

$$\frac{dw}{\cos(2\theta)} = \mathrm{d}r$$

larger footprint on the image plate at higher 2θ

'number of points (pixels) across the peak… is not changed' (Norby,1997).

When using focusing optics (von Dreele et al., 2006) the detector distance to the optics is fixed and the focal spot of the beam well below the PSF of the detector. The resolution is governed solely by the PSF of the detector.

PSF IP ~ 300 μm

von Dreele, R. B., Lee, P. L. & Zhang, Y. (2006) Protein polycrystallography. Zeitschrift für Kristallographie 23, 3-8.

Basic ideal geometry
finite beam

$$D\tan(2\theta+\mathrm{FWHM})=r+\Delta r$$

$$D\tan(2\theta+\mathrm{FWHM})=D\tan(2\theta)+\Delta r$$

$$\mathrm{FWHM}=\arctan(\tan(2\theta)+\frac{\Delta r}{D})-2\theta$$

$$\Delta r=\mathrm{PSF}*\frac{dw}{\cos(2\theta)}$$

If both Gaussian $\Delta r=\sqrt{\mathrm{PSF}^2+\frac{dw^2}{\cos^2(2\theta)}}$

FWHM

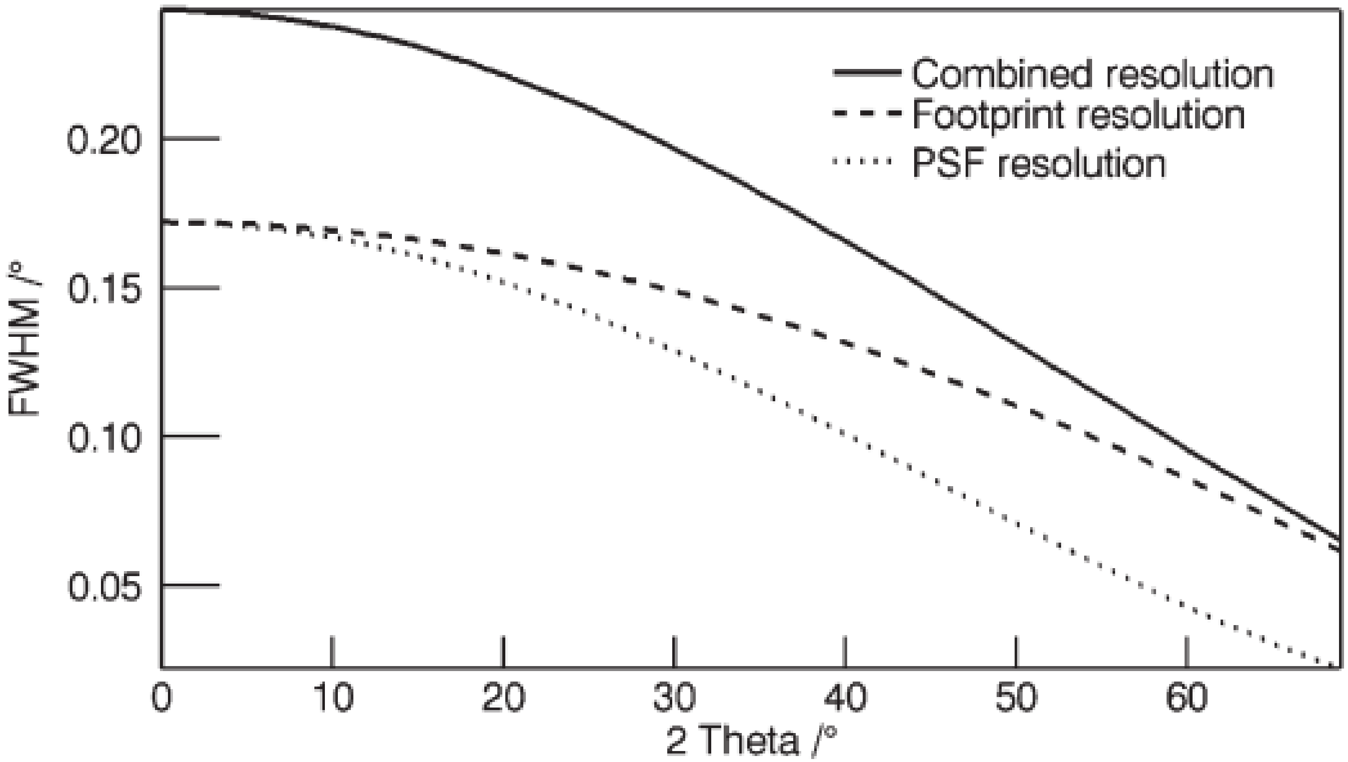

An example of the resolution contributions of an ideally aligned typical image plate detector placed 100 mm from the sample. The footprint of a 0.3 mm diffracted beam and the PSF of 0.3 mm of the detector contribute varying amounts to the resolution over the diffraction angle range.

Figure 14.4 Powder DiffractionTheory and Practice
BERND HINRICHSEN, ROBERT E. DINNEBIER AND MARTIN JANSEN

Area Detector comparison

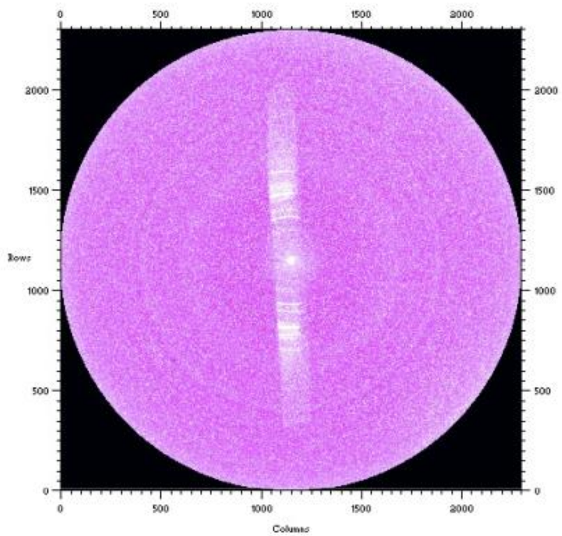

Mar345 IP detector

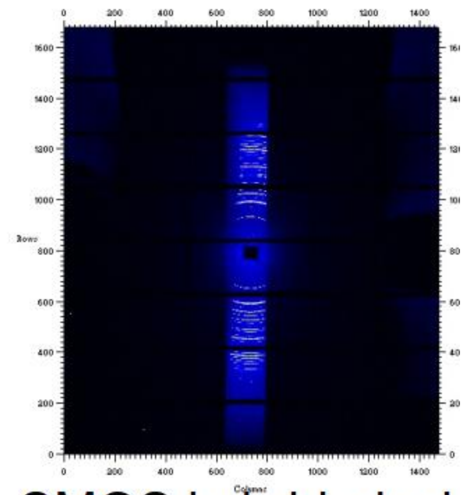

CMOS hybrid-pixel technology Pilatus 2M detector

Pilatus
pixel 172 μm
PSF 1 pixel

Mar345
pixel 172 μm
PSF 300 μm

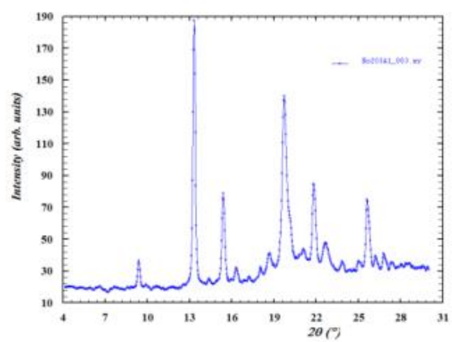

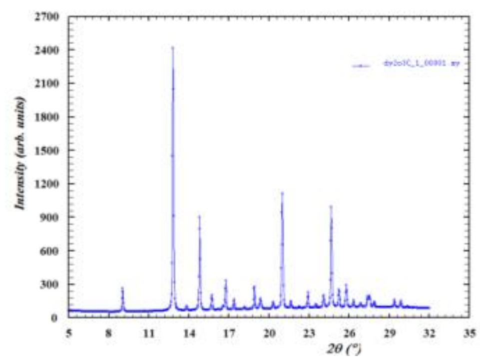

Tilted detector

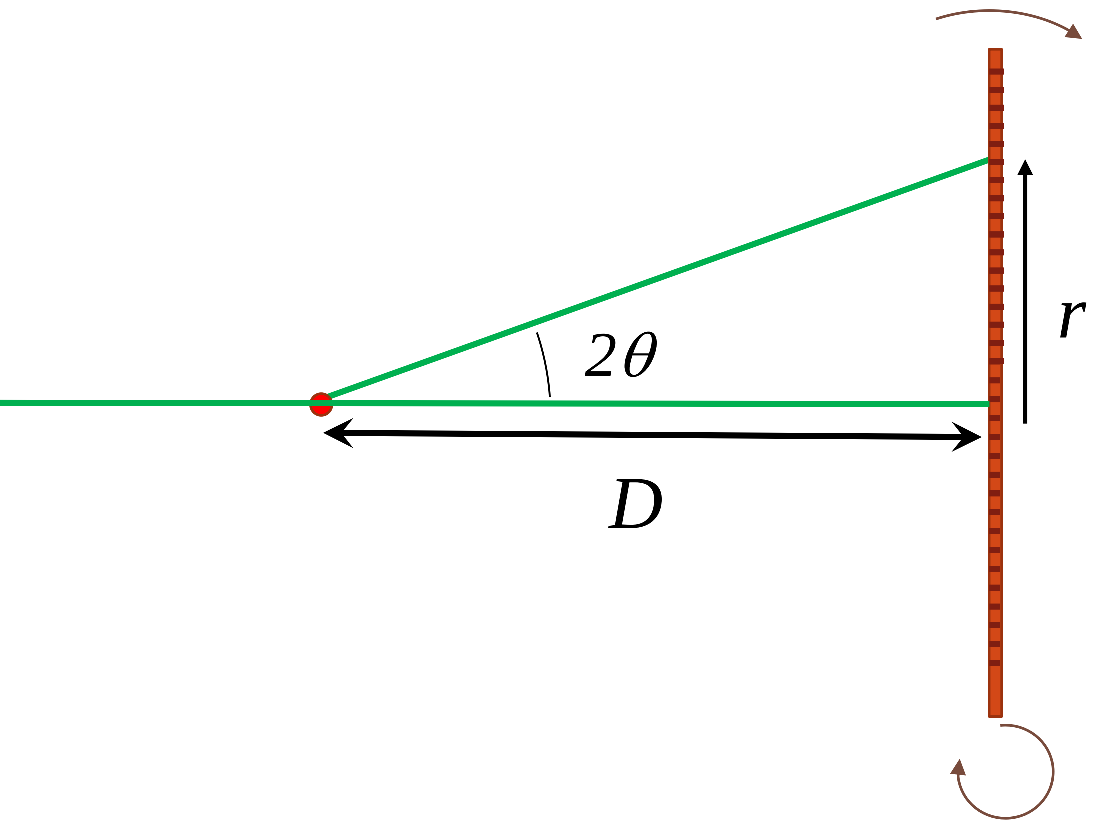

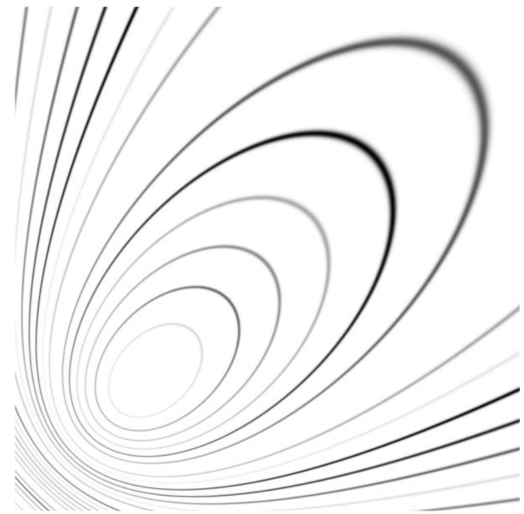
© powder3D_ip manual

Geometrical convention

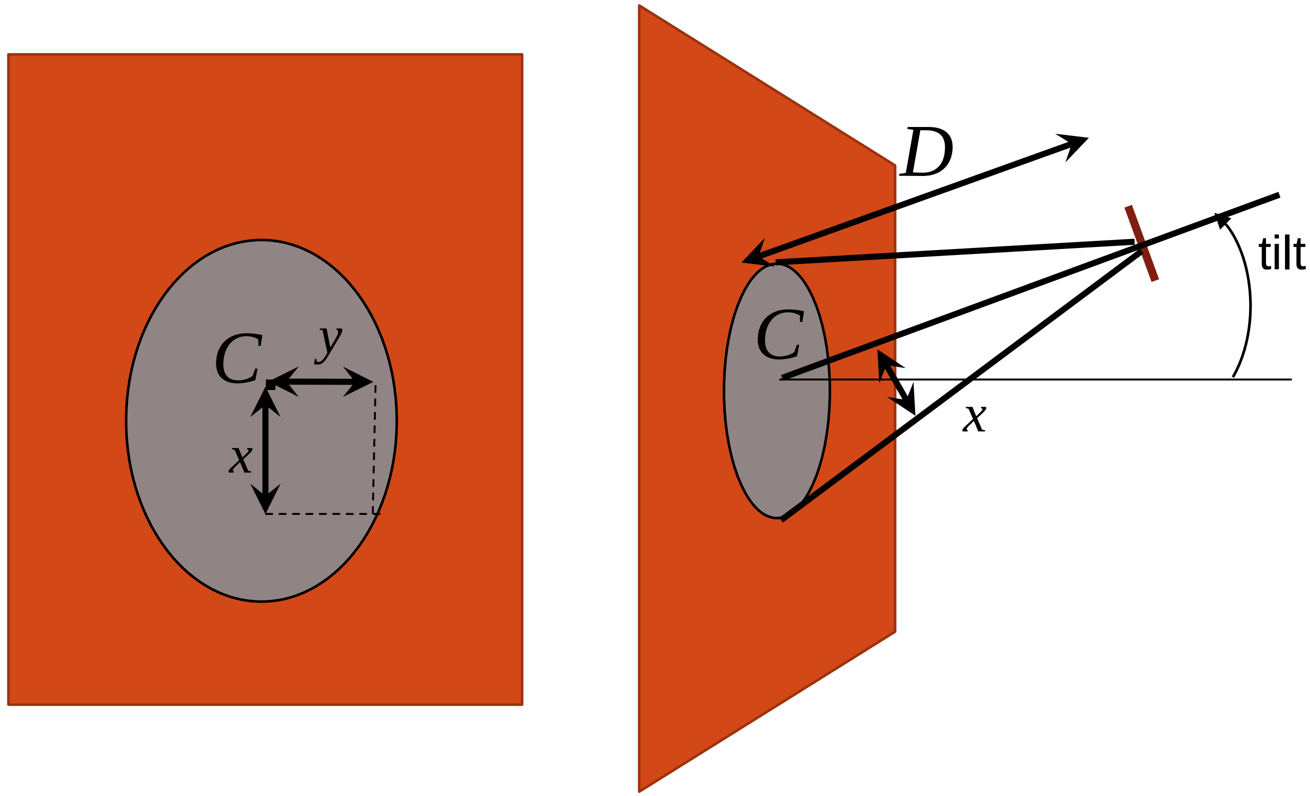

If the cone coordinate system are unaffected by detector tilt previous equation still keep when D is the distance between sample and the perpendicular plane respect cone axis in which points lay

$$D \tan 2\theta = r \quad \Rightarrow \quad x^2 + y^2 = D^2 \tan^2 2\theta$$

Diraction Angle Transformation

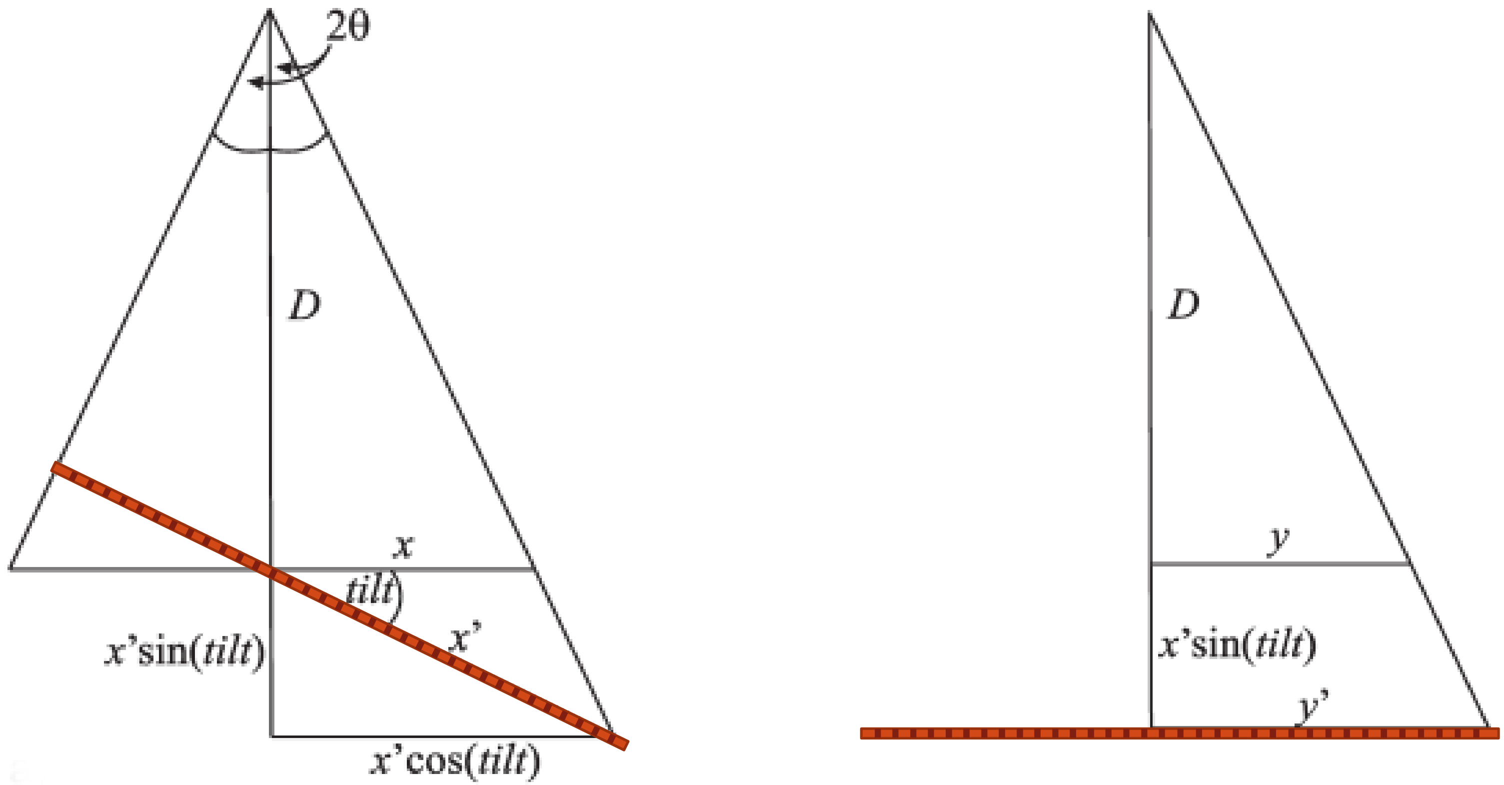

$$x^2 + y^2 = \left(\frac{Dx' \cos(tilt)}{D + x' \sin(tilt)}\right)^2 + \left(\frac{Dy'}{D + x' \sin(tilt)}\right)^2 = D^2 \tan^2 2\theta$$

$$x'^2 \cos^2(tilt) + y'^2 = (D + x' \sin(tilt))^2 \tan^2 2\theta$$

Figure: Kumar, A. (2006). thesis, Austin College
Formulas: Hammersley,A.P.et al(1996). High Pressure Research 14, 23-248.

Arbitrary tilt

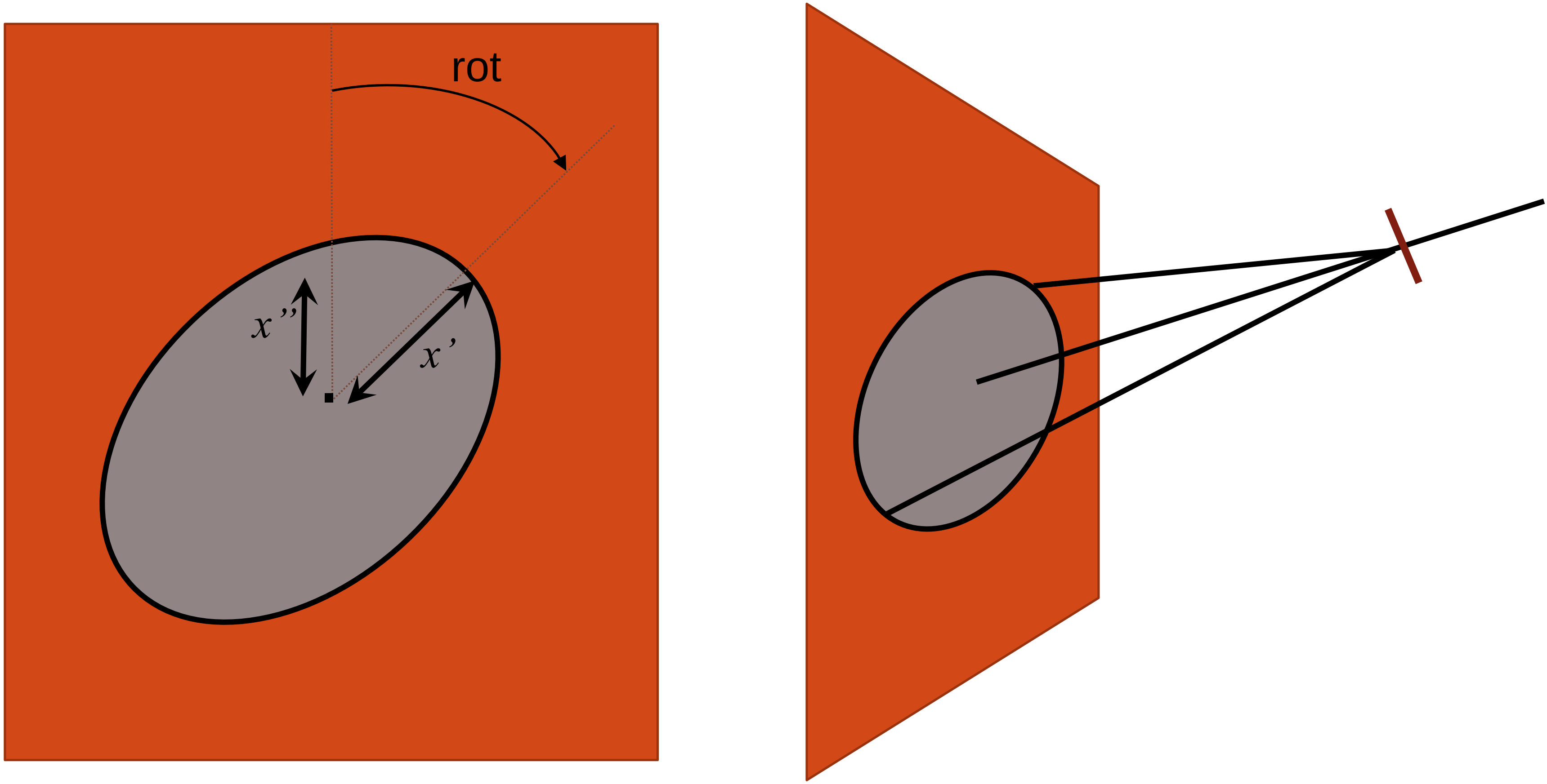

$$x' = x'' \cos(rot) + y'' \sin(rot)$$
$$y' = y'' \cos(rot) - x'' \sin(rot)$$

Arbitrary tilt

$$x' = x'' \cos(rot) + y'' \sin(rot)$$
$$y' = y'' \cos(rot) - x'' \sin(rot)$$

$$x'^2 \cos^2(tilt) + y'^2 = (D + x' \sin(tilt))^2 \tan^2 2\theta$$

$$(x'' \cos(rot) + y'' \sin(rot))^2 \cos^2(tilt) + (y'' \cos(rot) - x'' \sin(rot))^2$$
$$= (D + (x'' \cos(rot) + y'' \sin(rot)) \sin(tilt))^2 \tan^2 2\theta$$

$$2\theta = \arctan \sqrt{\frac{(x'' \cos(rot) + y'' \sin(rot))^2 \cos^2(tilt) + (y'' \cos(rot) - x'' \sin(rot))^2}{(D + (x'' \cos(rot) + y'' \sin(rot)) \sin(tilt))^2}}$$

General Transformations

- We know 2θ =f(D,tilt,rot,C,x,y)
- However we don't know *a priori* rot, tilt, D, C

We have an image with some ellipses from a standard

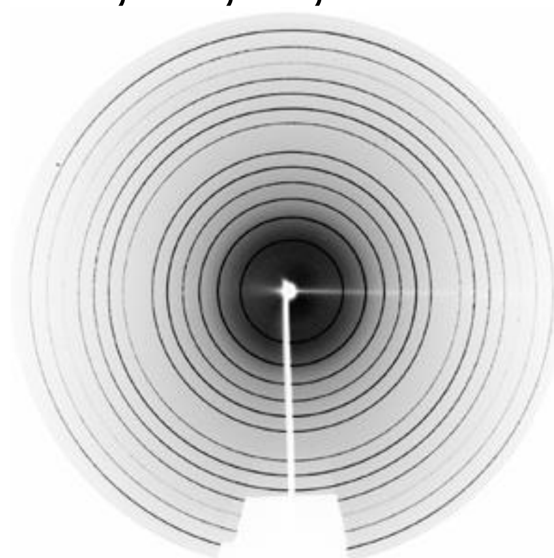

Sciences Chimiques de Rennes UMR CNRS 6226

General Transformations

a,b = semi-axes
l=semi-latus

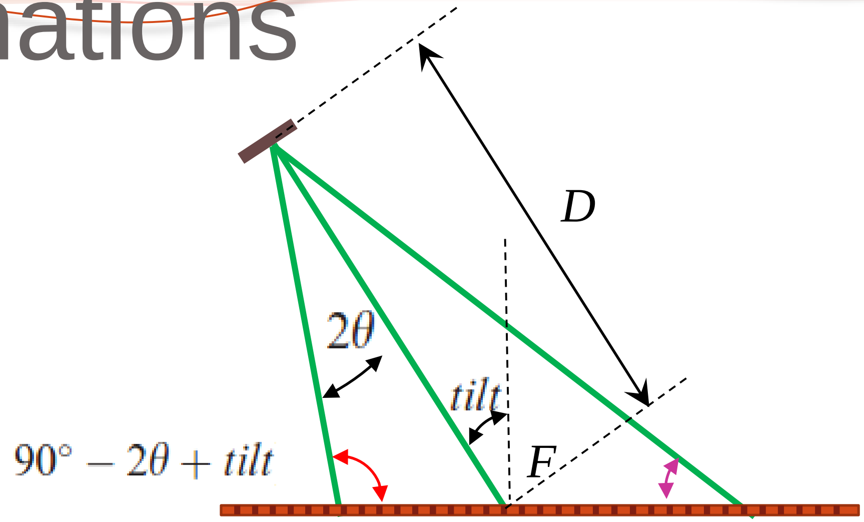

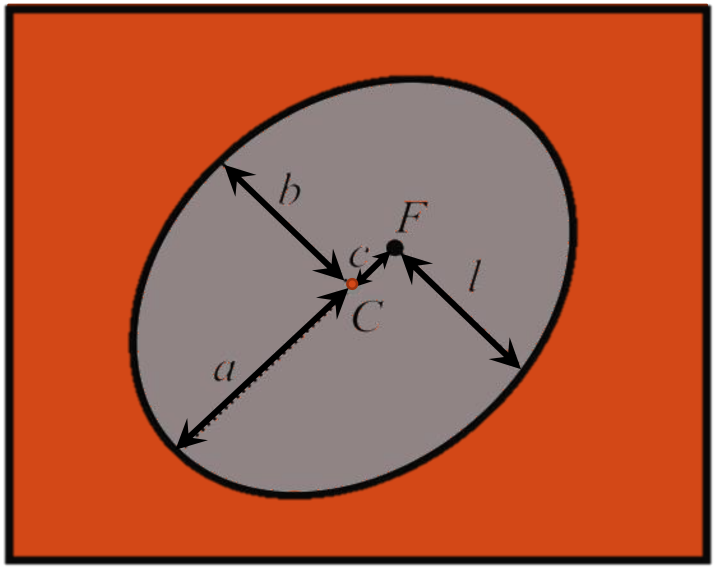

The semi-latus rectum ***l*** is independent of the tilt and only function of 2θ and detector distance

$$D \tan 2\theta = l$$

Using sine rule

$$\frac{\sin(2\theta)}{a+c} = \frac{\sin(90^\circ - 2\theta - tilt)}{D} \qquad c = -a + D\sec(tilt + 2\theta)\sin 2\theta$$

$$\frac{\sin(2\theta)}{a-c} = \frac{\sin(90^\circ - 2\theta + tilt)}{D} \qquad c = a - D\sec(tilt - 2\theta)\sin 2\theta$$

Sciences Chimiques de Rennes UMR CNRS 6226

HINRICHSEN thesis 2007 Universität Stuttgart

General Transformations

a,b = semi-axes
e=eccentricity
L=semi-latum

$$\frac{D\cos(tilt)\sin 4\theta}{\cos(2tilt)+\cos 4\theta} = a$$

$$\frac{2D\sin(tilt)\sin^2 2\theta}{\cos(2tilt)+\cos 4\theta} = c$$

$$D\tan 2\theta = l$$

Ellipses identity

$$al = b^2$$

$$e = c/a$$

$$e = \sqrt{1-\frac{b^2}{a^2}}$$

$$c = \sqrt{a^2-b^2}$$

$$\frac{D\sqrt{\cos(tilt)}\sqrt{\sin 2\theta}\sqrt{\tan 2\theta}}{\sqrt{\cos(2tilt)+\cos 4\theta}} = b$$

$$\tan(tilt)\tan 2\theta = e$$

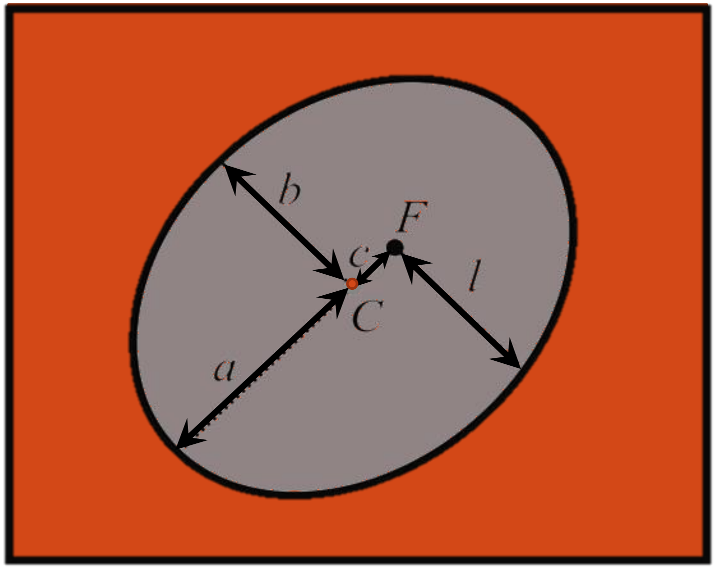

HINRICHSEN thesis 2007 Universität Stuttgart

Detector Coordinate Transformations

Ellipses identity

$$al = b^2$$

$$e = c/a$$

$$e = \sqrt{1 - \frac{b^2}{a^2}}$$

$$c = \sqrt{a^2 - b^2}$$

$$\frac{D\cos(tilt)\sin 4\theta}{\cos(2tilt) + \cos 4\theta} = a$$

$$\frac{D\sqrt{\cos(tilt)}\sqrt{\sin 2\theta}\sqrt{\tan 2\theta}}{\sqrt{\cos(2tilt) + \cos 4\theta}} = b$$

$$\tan(tilt)\tan 2\theta = e$$

$$r_{focus\ \ ellipse} = \frac{a(1-e^2)}{1 + e\cos(\alpha)} = \frac{D\tan 2\theta}{1 + \cos\alpha\tan(tilt)\tan 2\theta}$$

$$y_d = r_{focus\ \ ellipse}\sin(\alpha - rot)$$

$$x_d = r_{focus\ \ ellipse}\cos(\alpha - rot)$$

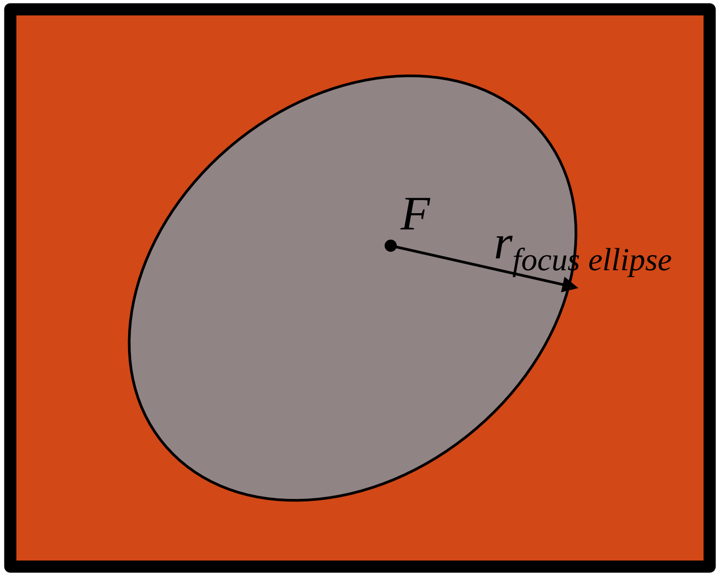

Intensity corrections

- Polarization correction
- Geometrical correction
- Lorentz correction

Polarization correction

- The polarization factor arises from partial polarization of the electromagnetic wave after scattering.
- Polarized beam can be represented by two components: $A_{\parallel}$ and $A_{\perp}$

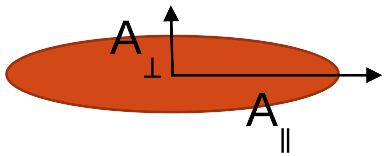

- The diffracted intensity is proportional to the square projections of εA on εk_{out}, (A^2 for $\varepsilon A \perp \Delta k$, $\cos^2(2\theta)A^2$)

- The overall intensity reduction of a not polarized beam scattered

$$P \propto \frac{1+\cos^2 2\theta}{2}$$

R. Kahn J. Appl. Cryst. (1982). 15, 330-337
Macromolecular Crystallography with Synchrotron Radiation: Photographic Data Collection and Polarization Correction

Polarization correction

the primary beam be polarized this changes the correction to

$$P = P_0 - P' \qquad P' = \frac{1}{2} J' \cos 2\alpha \sin^2 2\theta$$

Where α is the azimuthal angle, α=0 equatorial   J' is the degree of polarization

$$J' = (A_{\parallel} - A_{\perp}) / (A_{\parallel} + A_{\perp})$$

J'=1 ∥ polarization
J'=-1 ⊥ polarization
J'=0 no polarization

Sciences Chimiques de Rennes UMR CNRS 6226

R. Kahn J. Appl. Cryst. (1982). 15, 330-337
Macromolecular Crystallography with Synchrotron Radiation: Photographic Data Collection and Polarization Correction

Polarization correction

$$P = P_0 - P'$$

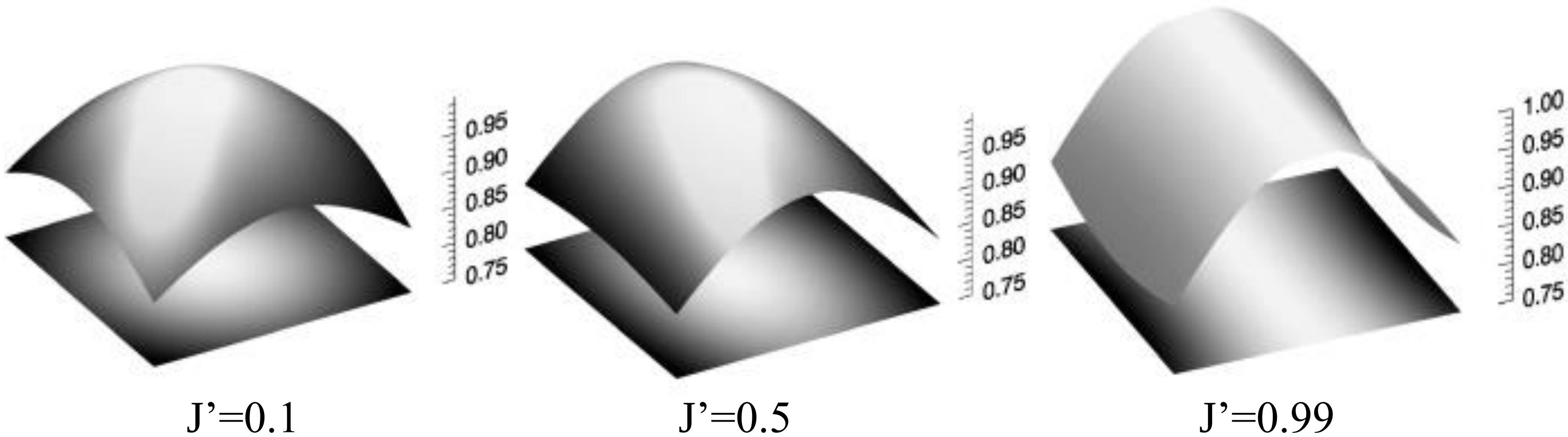

Two dimensional polarization correction for an ideally aligned detector. The correction is applied by dividing the intensities by the displayed correction values.

Figure 14.14 Powder DiffractionTheory and Practice
BERND HINRICHSEN, ROBERT E. DINNEBIER AND MARTIN JANSEN

Geometrical correction

- Change of solid angle cover by a pixel

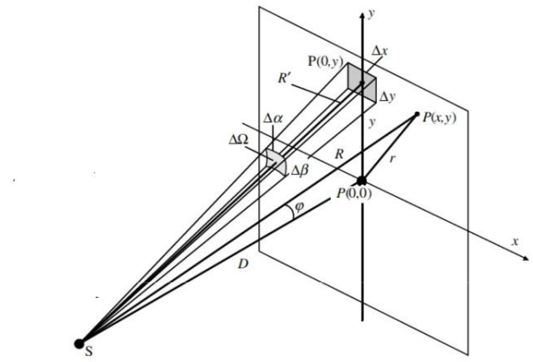

- partial transmission of X-ray trough the active layer
  Optic path in the active layer

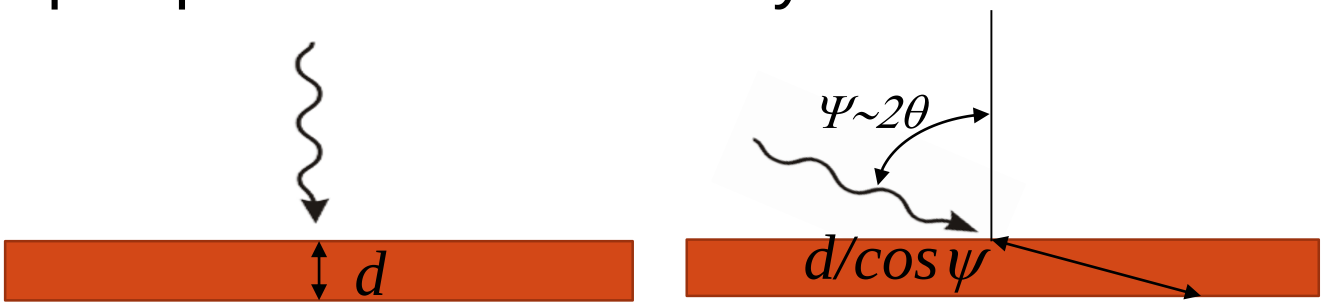

Geometrical correction

- Change of solid angle cover by a pixel

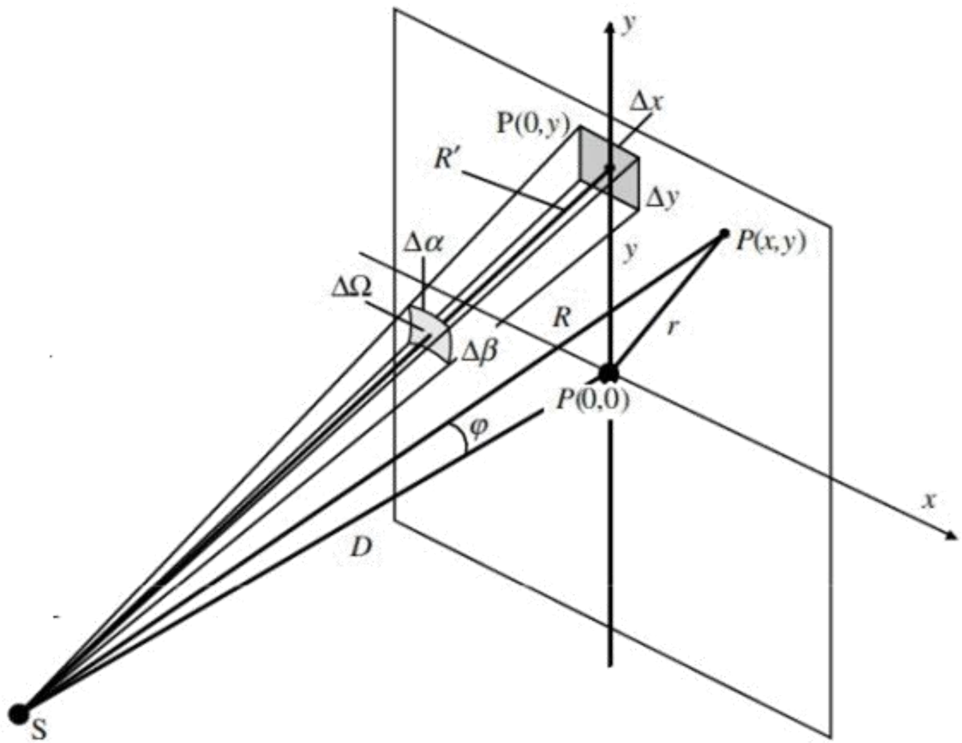

$$\Delta\beta = \frac{D}{D^2 + y^2}\Delta y = \frac{D}{R'^2}\Delta y \qquad \Delta\alpha = \frac{\Delta x}{R'}$$

$$\Delta\Omega = \Delta\beta\Delta\alpha = \frac{D}{R'3}\Delta A$$

$$Flux\ for\ pixel \propto \Delta\Omega$$

$$K = \frac{Flux(\mathrm{x,y})}{Flux(0{,}0)} = \frac{D^3}{R'3} = cos^3\Psi \cong cos^3 2\theta$$

Implemented on fit2D
geometrical correction to intensity

Geometrical correction

- K is the angular dependent detector efficiency

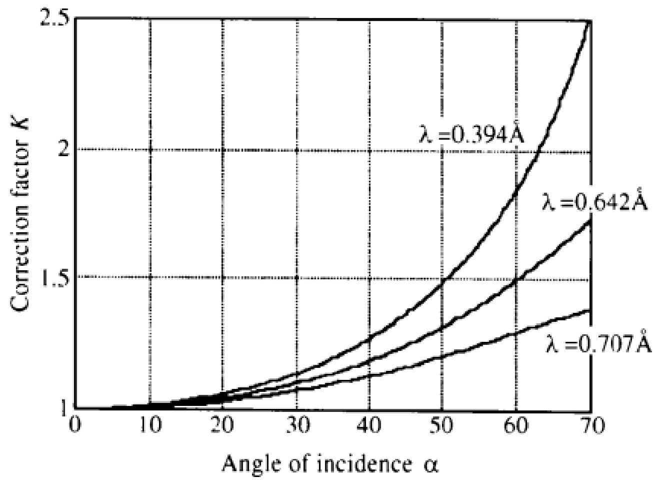

Fig. 2. Correction factor K for three different wavelengths, such $I_{corr} = I_{obs}/K$.

$$K = \frac{1 - e^{-\frac{\mu d}{\cos 2\theta}}}{1 - e^{-\mu d}} = \frac{1 - e^{-\frac{\ln T_{\perp}}{\cos 2\theta}}}{1 - T_{\perp}}$$

$$I_{corr} = {I_{obs}}/{K}$$

Implemented in Fit2D inside flat field correction

J. Zaleski, G. Wu and P. Coppens, J. Appl. Crystallogr., 1998, 31, 302–304

Lorentz correction

For Debye-Scherrer and Bragg-Brentano classical term implemented in Rietveld software (ignoring all constants)

$$L = \frac{1}{\sin\theta \sin 2\theta} \quad \text{or} \quad \frac{1}{\sin^2\theta \cos\theta}$$

This factor include 3 effect

- Statistic
- Slits acceptance
- Angular velocity

Lorentz correction statistic and slits factor

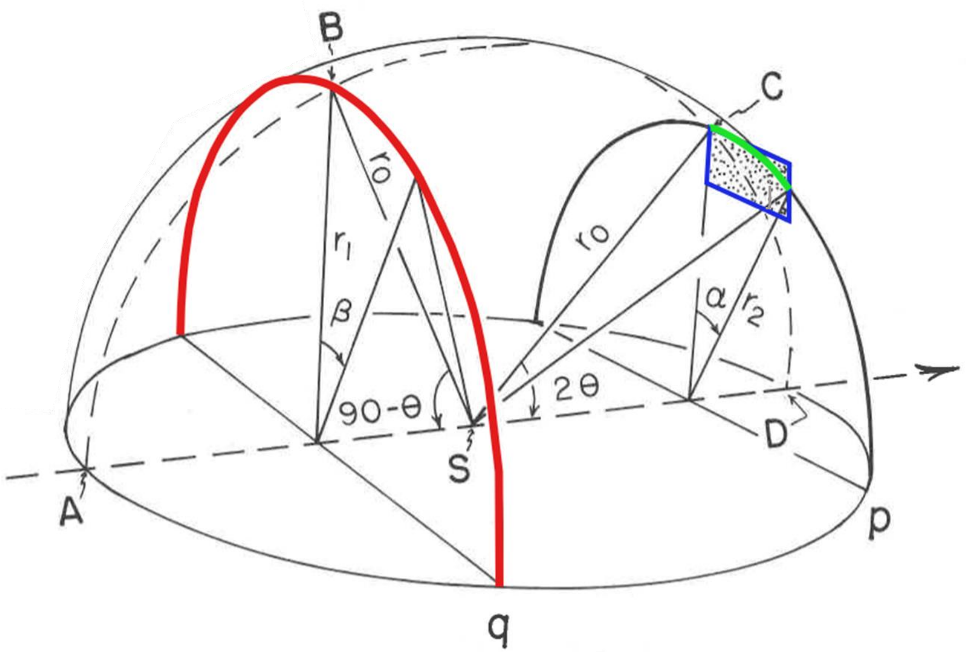

Crystallite in diffraction condition
∝B arc ∝ sin 90-θ=cos θ

Slits acceptance
$\propto\alpha = \arcsin({}^{j}/_{r_0 sin2\theta}) \cong {}^{j}/_{r_0 sin2\theta}$

$$Lp \propto {}^{cos\theta}/_{sin2\theta} = {}^{1}/_{2sin\theta}$$

Sciences Chimiques de Rennes UMR CNRS 6226

Reynolds, R. C *American Mineralogist* 61, no. 5–6 (June 1, 1976): 484–91.

Single crystal angular velocity

For Debye-Scherrer (equatorial scan) Ewald sphere velocity reduces to Darwin form

$$L \approx {}^{1}/_{sin2\theta}$$

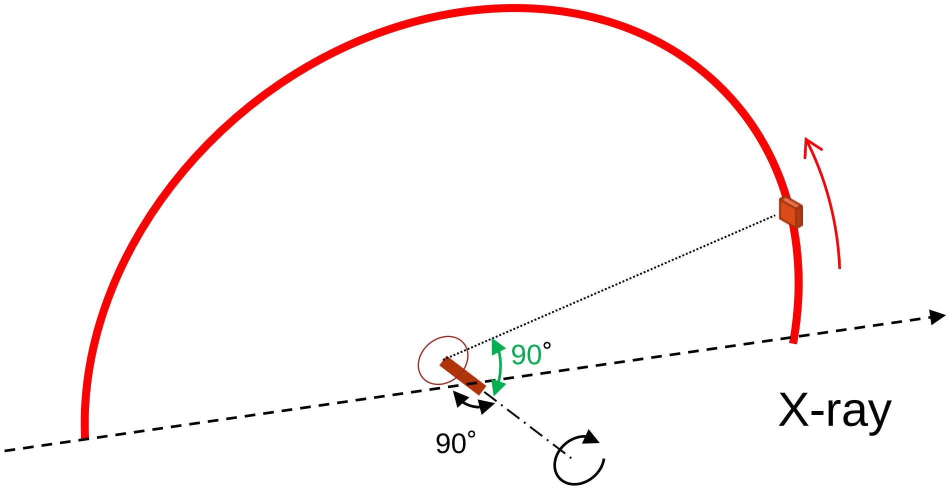

But for two dimensional detector the angle between sample axis rotation and detector plane is different from 90°

Darwin, C. G., "Reflection of X-Rays from Imperfect Crystals," Phil. Mag.,43, (1922).

Non equatorial Lorentz correction

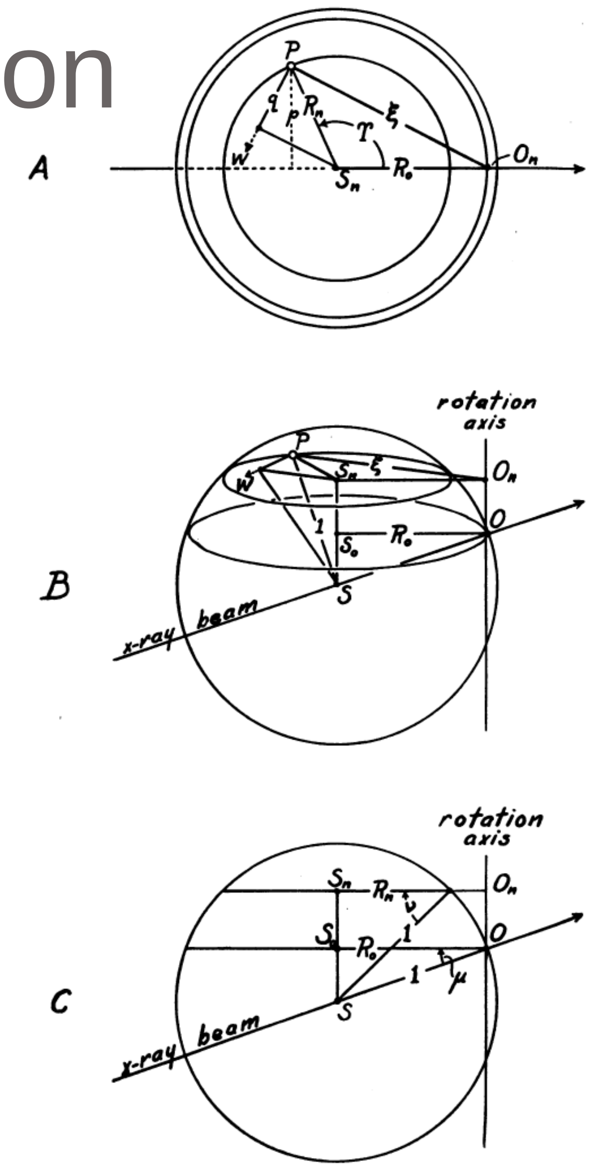

FIGURE 1

$$L \sim \frac{1}{\cos\mu \cos\nu \sin\Upsilon}.$$

μ angle between axis of sample rotation and plane ⊥ beam
γ and ν horizontal and vertical reflection displacement

Buerger, M. J. "The Correction of X-Ray Diffraction Intensities for Lorentz and Polarization Factors." *PNAS* 26, no. 11 (1940): 637.

Non equatorial Lorentz correction

Expressed in terms of azimuthal angle

$$L^{-1} = \cos\mu \frac{\cos\alpha \tan 2\theta}{\sqrt{1+\cos^2\alpha \tan^2 2\theta}\sqrt{1+\sin^2\alpha \tan^2 2\theta}}$$

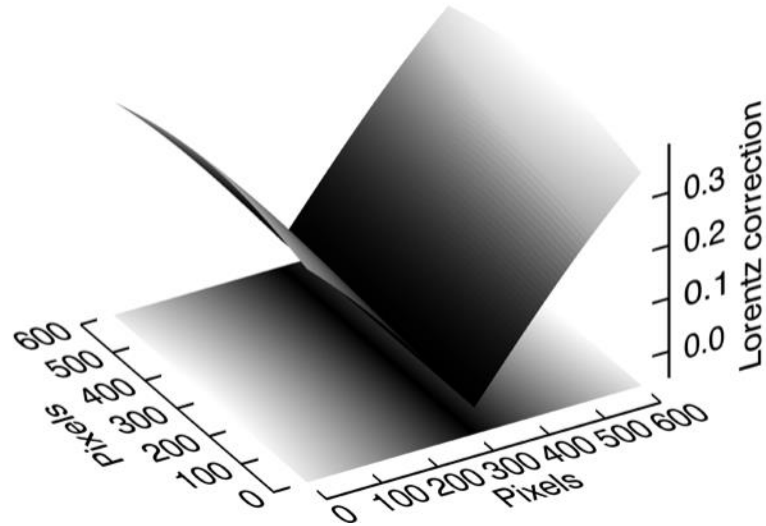

The two-dimensional single crystal Lorentz correction for an ideally aligned detector. Note the zero values in the central valley. These cause divergent intensities as they are multiplied with the inverse of the Lorentz correction. Therefore the intensities in that region have no meaning. The central valley is parallel to the sample rotation axis.

Although Fit2D documentation is not clear if apply the azimuthal dependent Lorenz correction is clearly state that intensity are renormalized by a sin2θ factor to maintain compatibility with current Rietveld software

Pre treatment of the data

- Several region should be rejected from integration:
  - Beam stop
  - Bad pixel (dust grain, damaged pixel, etc)
  - Dead zone
  - Saturating spot (big crystallite or cluster of orietered crystallite)
- Manually selecting polygons, arcs, circles
  - Fit2D
- Automatic setting threshold on intensity or filtering the distribution

Calibration

- Definition of a set of d-spacing for calibration image
- Definition of the direct beam position center of circle in orthogonal detector
- Definition of ellipses and experimental geometry
- Refinement
- Azimuthal check

Center determination

- User assisted method (Fit2D)
  - Direct beam trace (semi opaque beam stop)
  - Circle or ellipse center (click on ellipse)
  - Fit projection
- Fully automatic
  - Cervellino method: minimize the inverse normalized variance of the radial distribution function.
  - Powder3D_IP Intersection of mirror plane for vertical and horizontal cut (need center to be in the plate)

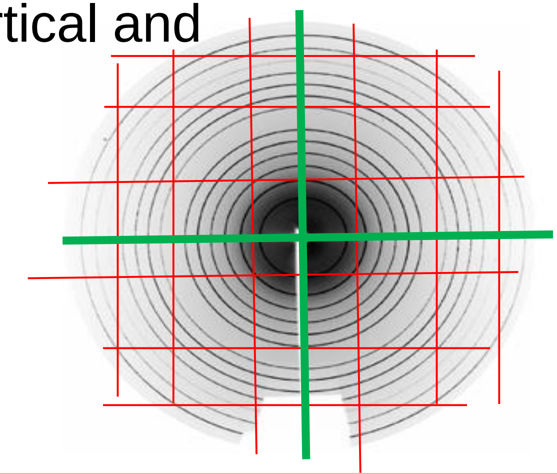

Tilt and rotation

- Fit2D: manual fit of several ellipses

- Powder 3D: automatic fit with the Hough transform, as has been described by Rajiv and by Fisker

Rajiv, P., Hinrichsen, B., Dinnebier, R., Jansen, M. & Joswig, M. (2007) Powder Diffraction 22.

Fisker, R., Poulsen, H. F., Schou, J., Carstensen, J. M. & Garbe, S. (1998) J. App. Cryst. 31, 647-63.

Refinement

- The radial line intersection method
  Fit2D, Powder3D, Maud

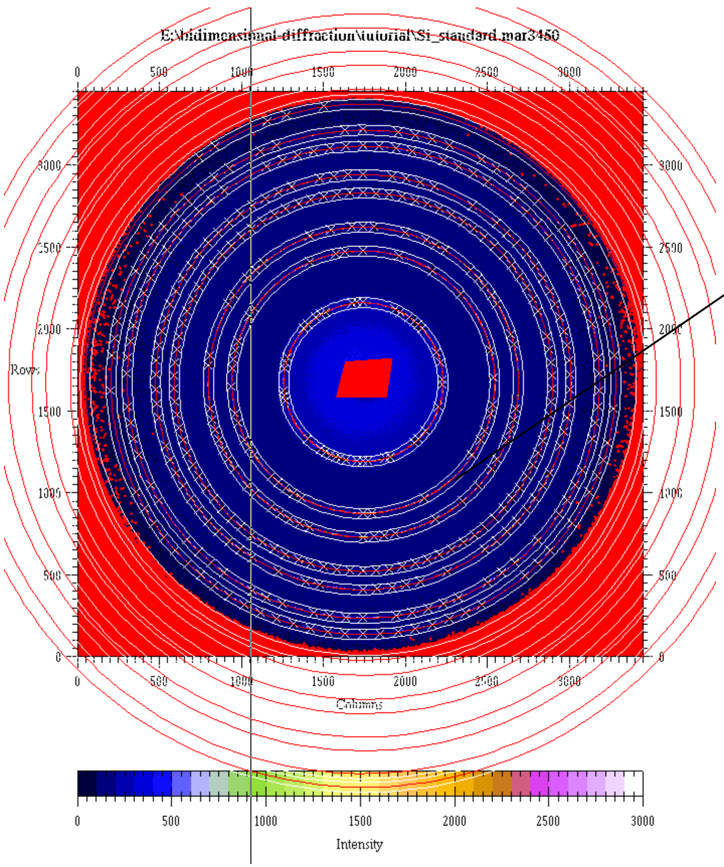

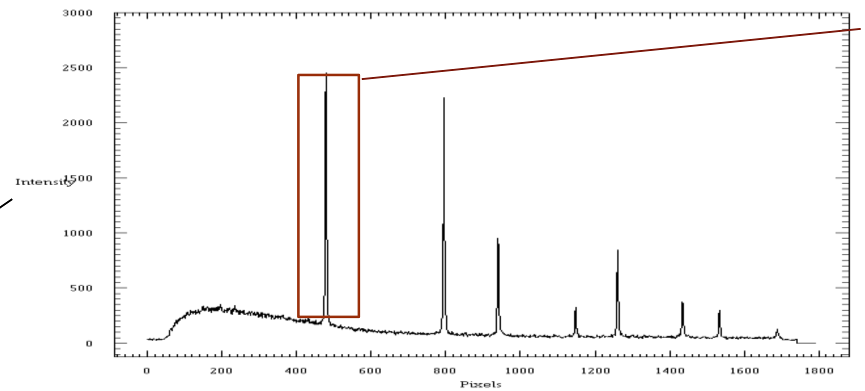

Gaussian fit

Several slice are cut starting from the approximated center (bins) and successively fitted in terms of center, tilt detector distance etc.

$$r_{focus-ellipse} = \frac{D\tan 2\theta}{1+\cos\alpha\ \tan(tilt)\tan 2\theta} \qquad w_i = D\sin 2\theta$$

Sciences Chimiques de Rennes UMR CNRS 6226

Whole image refinement

- Powder3D_IP: the entire image is reconstructed and subtracted from the measured image. This difference is weighted and used as the residual for the refinement process.

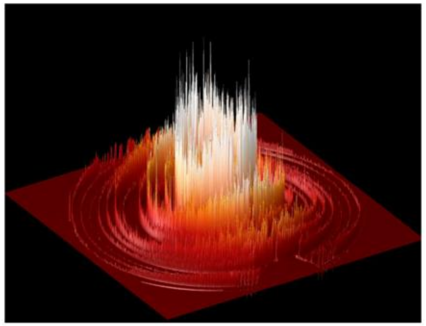

exp

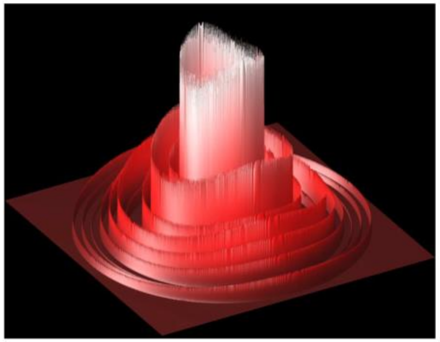

fit

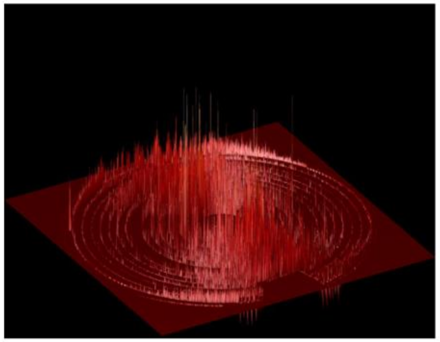

residual

Comparison of methods for no tilt

Software/method	X0[pixels]	Y0[pixels]	Tilt[°]
Real Values	1150	1150	0
Fit2D (traditional)	1150	1150	7.60E-07
Powder3D (traditional)	1150.001	1150.0007	-0.00020402
Powder3D WIR 10*10 binning	1149.9966	1149.9971	-0.000687
Powder3D WIR 2*2 binning	1150.0007	1150.0001	-0.000104
Powder3D WIR no binning	1150.0005	1150	-0.00010347
	Distance[mm]	Wavelength[Å]	Chi²
Real Values	100	1	
Fit2D (traditional)	99.99296	1.000053	4.92E-07
Powder3D (traditional)	100.00384	0.99998171	1.89E-07
Powder3D WIR 10*10 binning	99.999813	0.999989	4.90E-07
Powder3D WIR 2*2 binning	99.999886	0.999999	1.14E-08
Powder3D WIR no binning	99.999881	0.99999842	1.11E-08

Integration

- In the idea that detector doesn't move: however if you cliche is not too spotty you can still refine tilt and center Just press a button
- Two options:
  - Full ring integration (high statistic)
  - Multiple azimuthal bin texture studies
- Take care of consistency between correction done by integration software and rietvend program.

Final consideration

- Trash in, trash out:

if collection on the calibrant is bad
calibration in bad and integration on sample is worst

Less is better : don't hesitate to use masking if calibration is reasonable

Fit2D

- The software is composed of a graphical windows and a shell where information appear and command line mode could activated

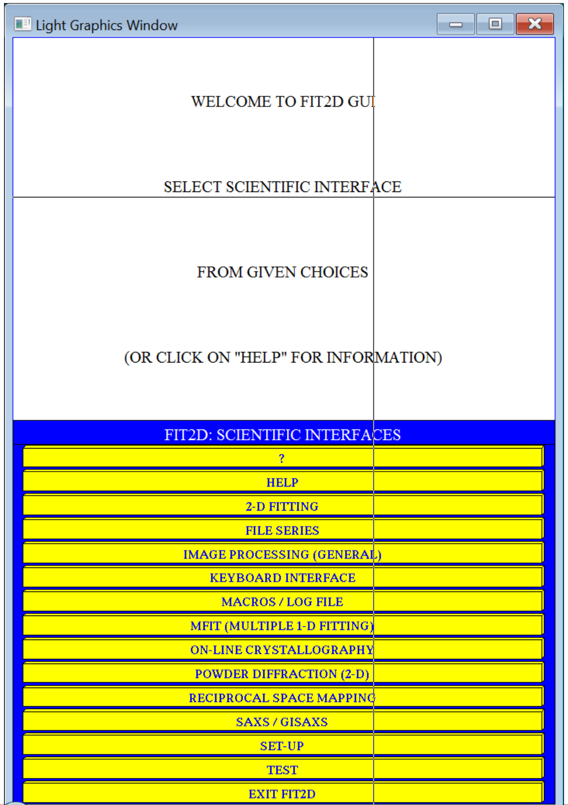

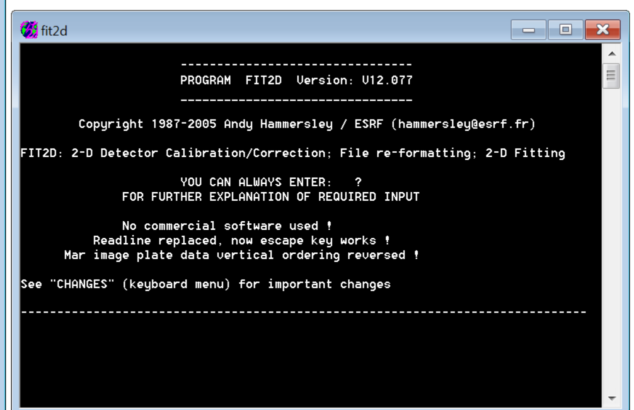

+Very flexible
+Open a lot of image kinds
+widely available linux win mac

-obscure documentation
-not frequently update
-limited choice of option

Start

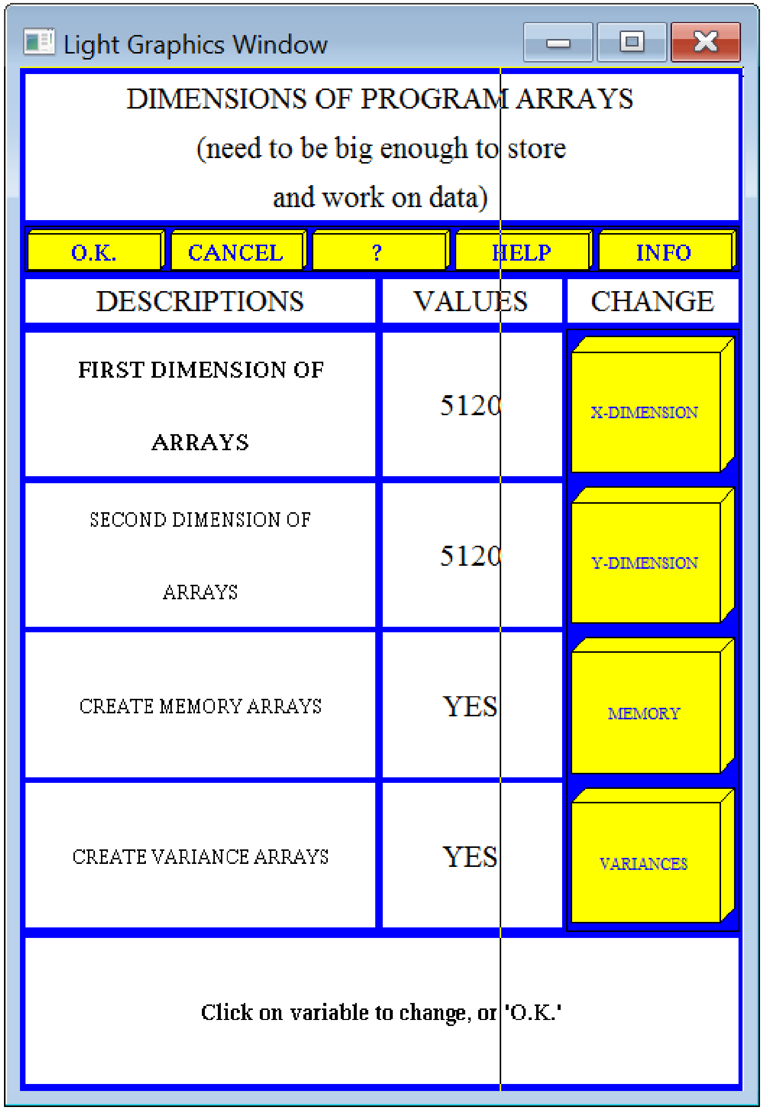

Define the image array size at list the number of pixel in the image

Use of memory array on actual computer doesn't matter any limit consideration

Keep track of variance during manipulation

Start

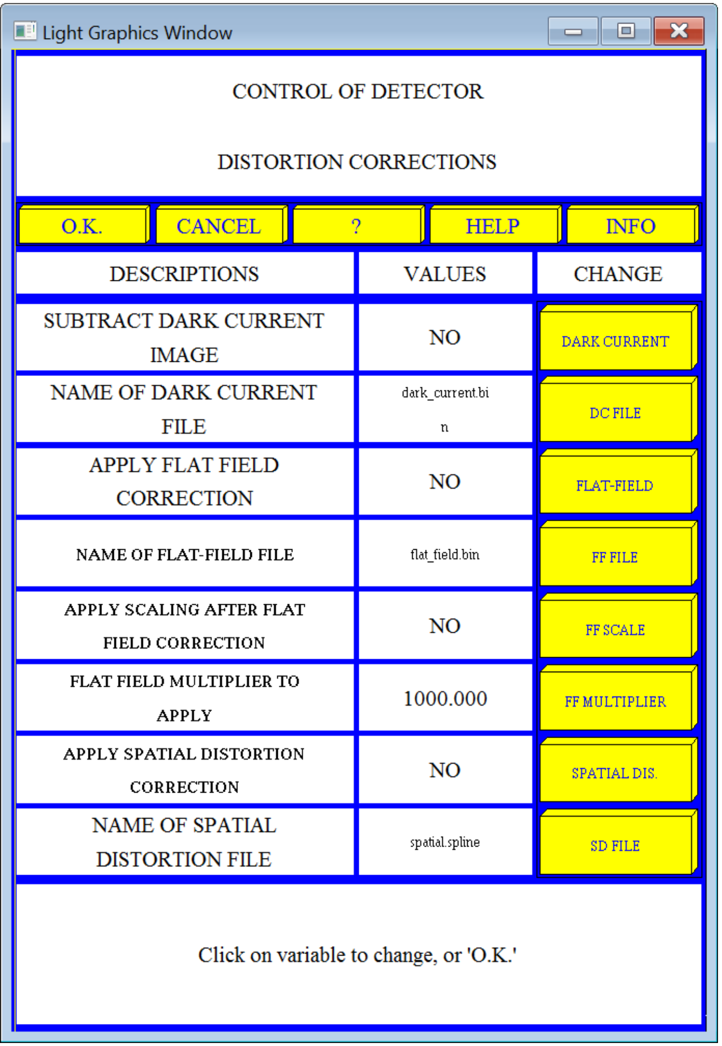

Light Graphics Window

CONTROL OF DETECTOR

DISTORTION CORRECTIONS

O.K. | CANCEL | ? | HELP | INFO

DESCRIPTIONS	VALUES	CHANGE
SUBTRACT DARK CURRENT IMAGE	NO	DARK CURRENT
NAME OF DARK CURRENT FILE	dark_current.bin	DC FILE
APPLY FLAT FIELD CORRECTION	NO	FLAT-FIELD
NAME OF FLAT-FIELD FILE	flat_field.bin	FF FILE
APPLY SCALING AFTER FLAT FIELD CORRECTION	NO	FF SCALE
FLAT FIELD MULTIPLIER TO APPLY	1000.000	FF MULTIPLIER
APPLY SPATIAL DISTORTION CORRECTION	NO	SPATIAL DIS.
NAME OF SPATIAL DISTORTION FILE	spatial.spline	SD FILE

Click on variable to change, or 'O.K.'

- Principal correction
- Dark current image (subtract image)
- Flat field (multiplier image)
- Spatial distortion (spline deforming the image) can include detector transparency

Start

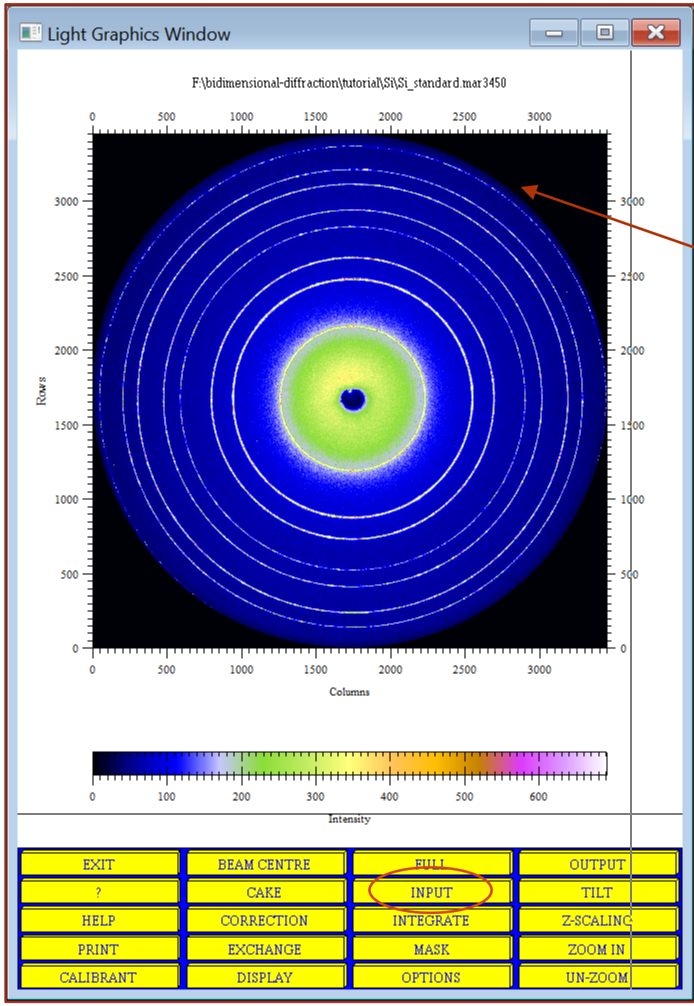

Just press input and navigate in the menu

Empty region

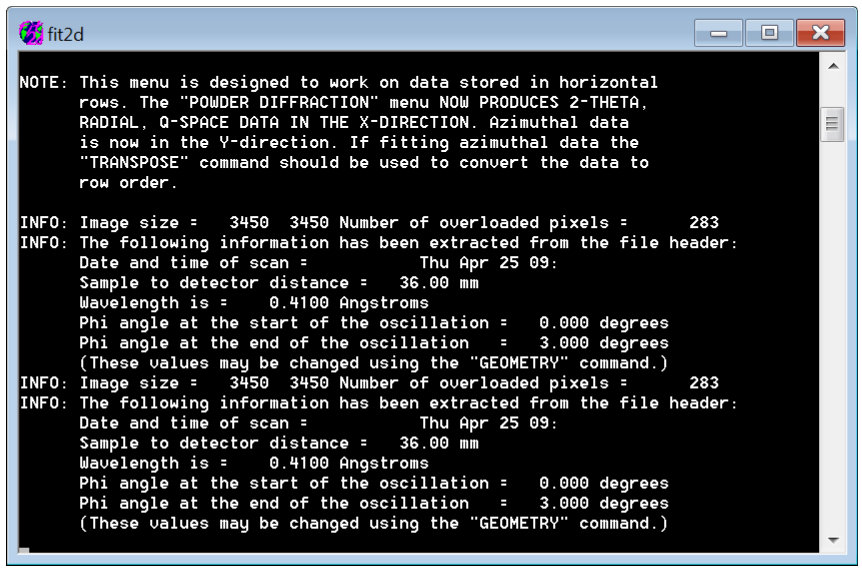

Z-scaling

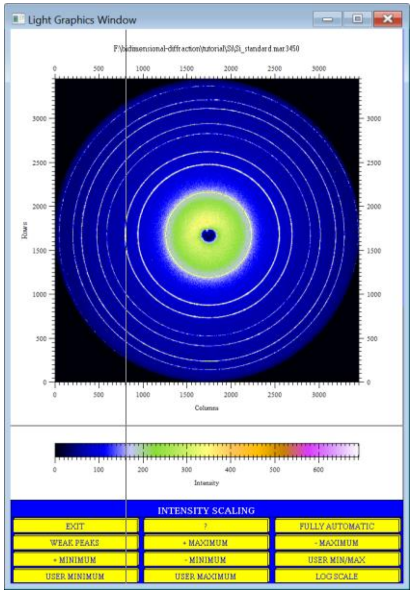

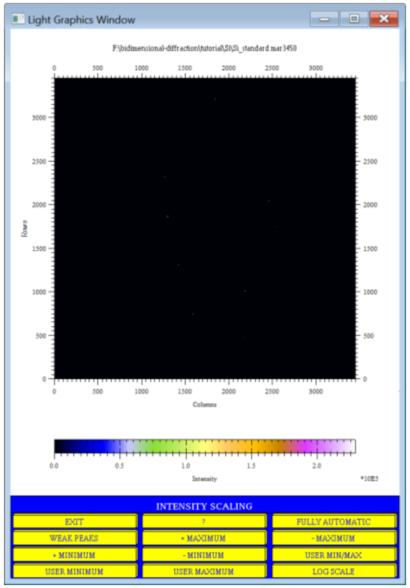

Weak peaks

Fully automatics

- Define color code for intensity fundamental to discover aberration and outliner

Need to mask something

Sciences Chimiques de Rennes UMR CNRS 6226

Mask

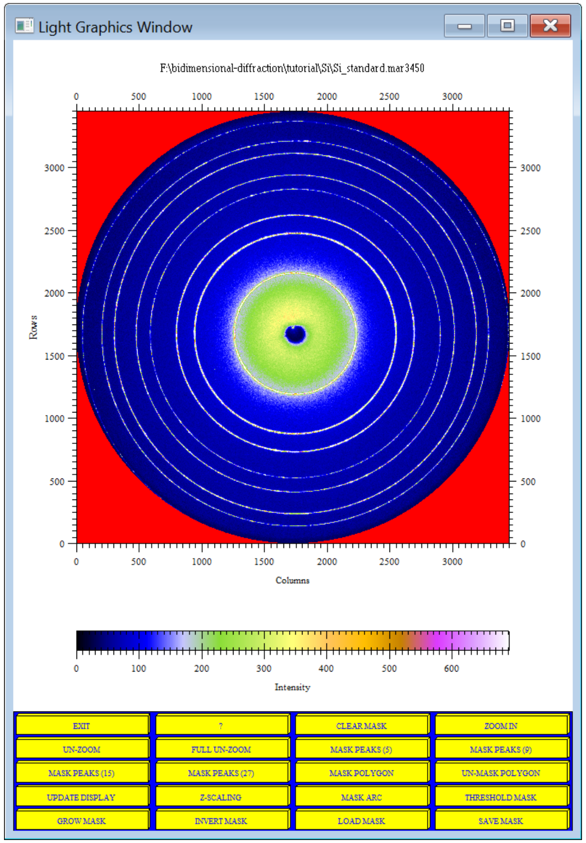

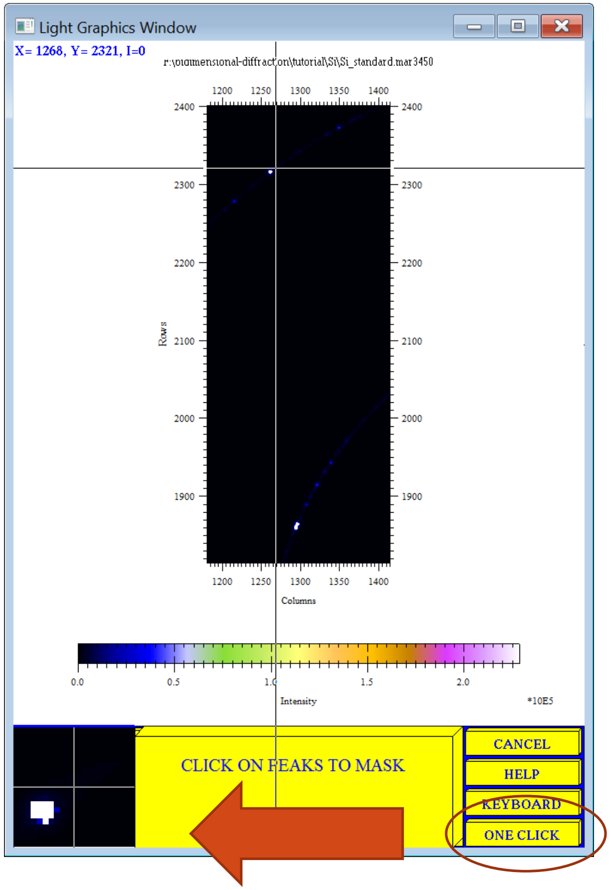

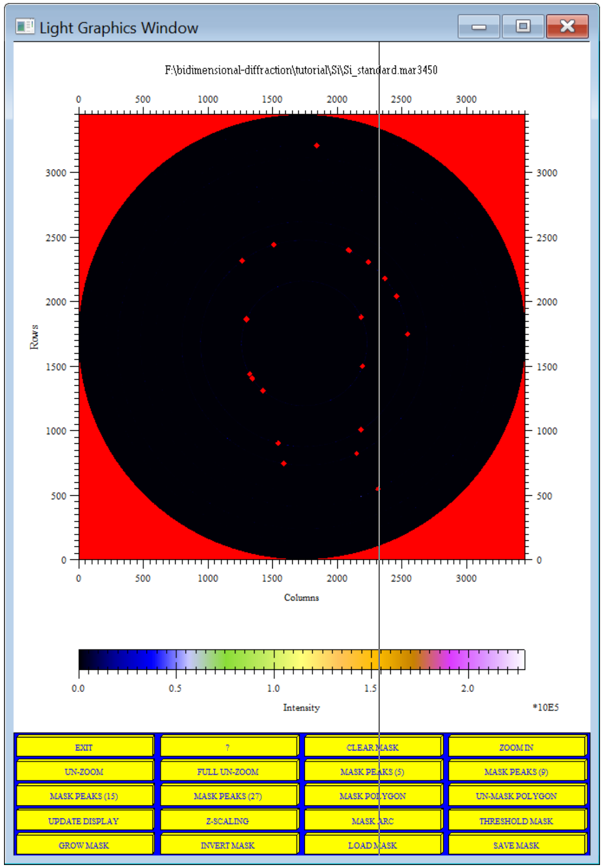

Low threshold mask

Fully masked image

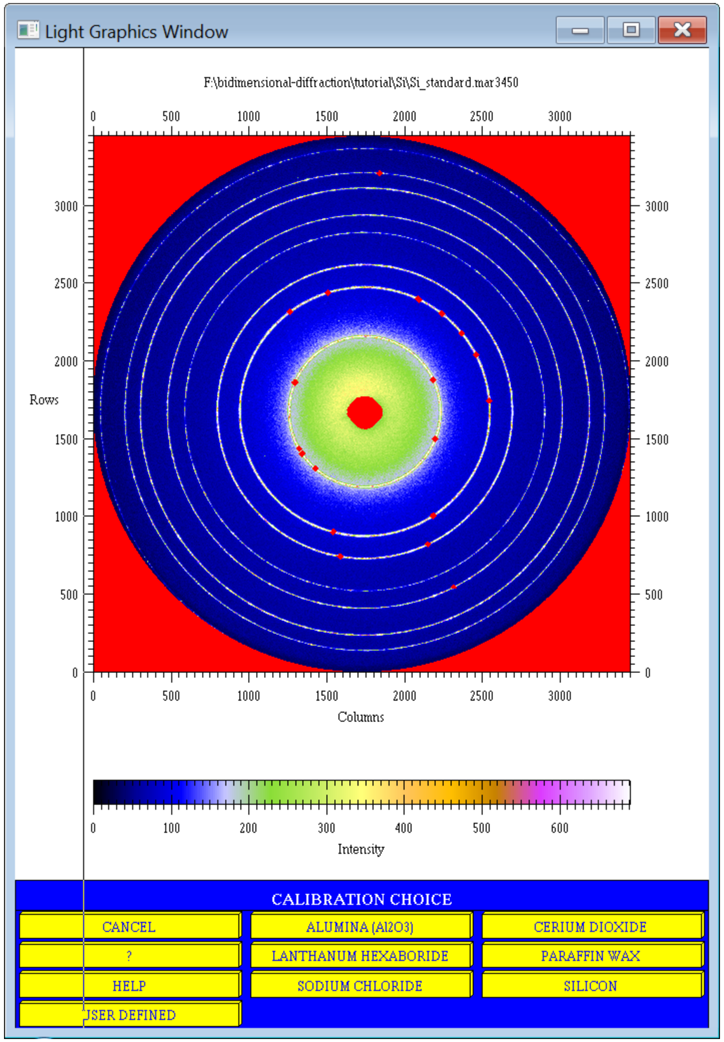

- Calibrant menu

  set of standard compound for calibration

  User could use a custom calibrant need a list of d-spacing in a text file

  In our case Si

Sciences Chimiques de Rennes UMR CNRS 6226

Calibrant

O.K.	CANCEL	?	HELP	INFO

DESCRIPTIONS	VALUES	CHANGE
SAMPLE TO DETECTOR DISTANCE (MM) (STARTING)	36.00000	DISTANCE
WAVELENGTH (ANGSTROMS) (STARTING)	0.124619	WAVELENGTH
SIZE OF HORIZONTAL PIXELS (MICRONS)	100.0000	X-PIXEL SIZE
SIZE OF VERTICAL PIXELS (MICRONS)	100.0000	Y-PIXEL SIZE
NUMBER OF AZIMUTHAL SECTIONS	360	ANGULAR SECTIONS
REJECT OUT-LYING POSITIONS AND RE-REFINE	YES	REJECT OUTLIERS
REJECT LIMIT FROM IDEAL (STANDARD DEVIATIONS)	4.000000	REJECT LIMIT
OUTPUT FULL INFORMATION	YES	FULL INFO
REFINE X/Y BEAM CENTRE	YES	REFINE BEAM X/Y
REFINE SAMPLE TO DETECTOR DISTANCE	YES	REFINE DISTANCE
REFINE X-RAY WAVELENGTH	NO	REFINE WAVELENGTH
REFINE DETECTOR NON-ORTHOGONALITY	YES	REFINE TILT
FIT INTERMEDIATE NUMBER OF RINGS	YES	EXTRA ITERATIONS

- Approximate sample to detector distance
  nobody knows where is the active layer
- Wavelengths precise a possible
- Pixel size
- Number of azimuthal section
  number of slice used to refine the geometry stat with few (90) and repeat with 360
- Reject outline Yes but depends
- Refine beam center Yes
- Refine sample to detector distance Yes
- Refine wavelength NO correlate with distance
- Refine Tilts Yes
- Fit intermediate number of ring Depends

Center of the beam

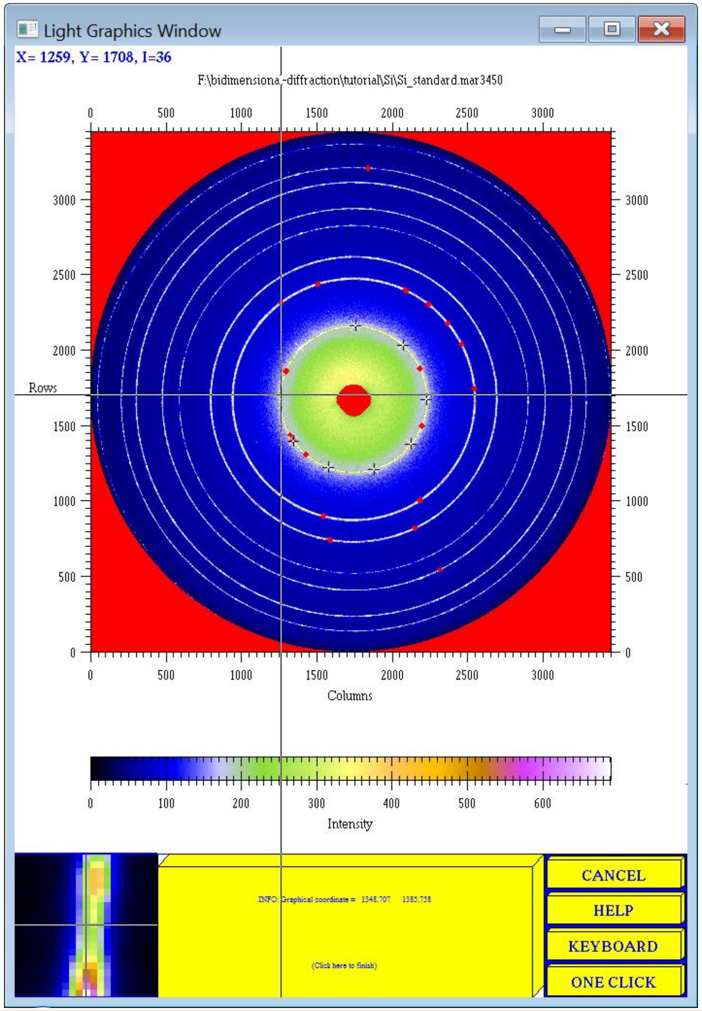

- Indicate first circle position click all around if circle s not compleat search to use the largest path
- Use two click
- If using user calibrant is better to write in the file the first intense reflection d-spacing

Refinement

- Poor starting value….

  But better values are estimated is shell windows

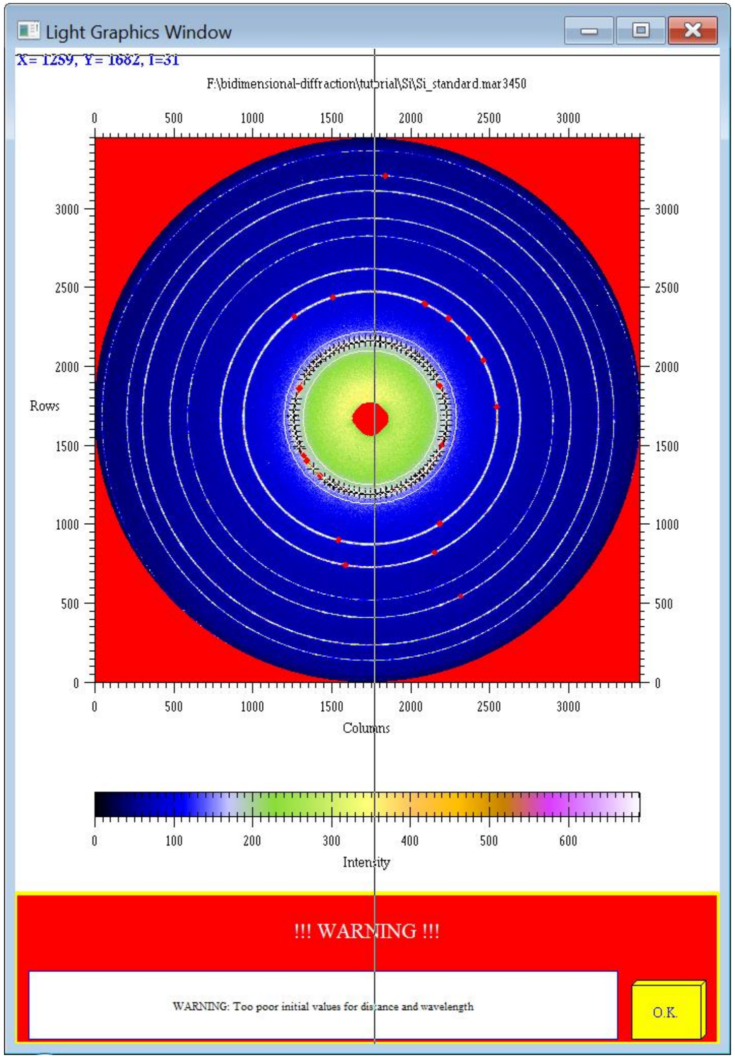

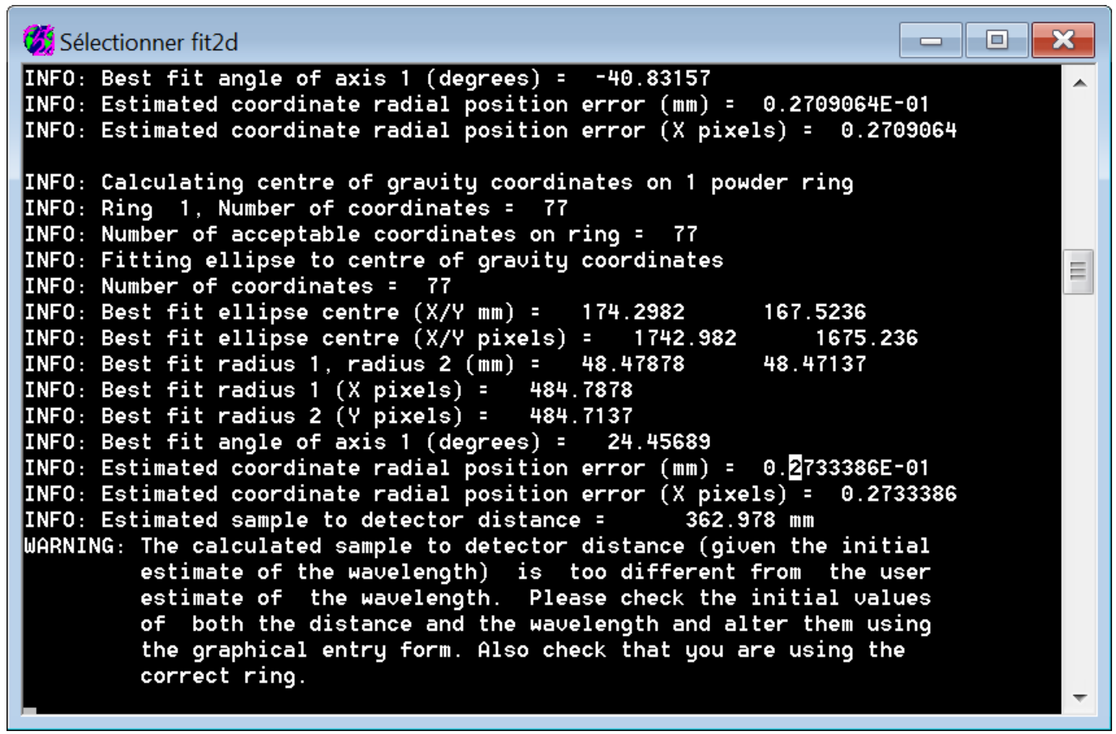

calibration

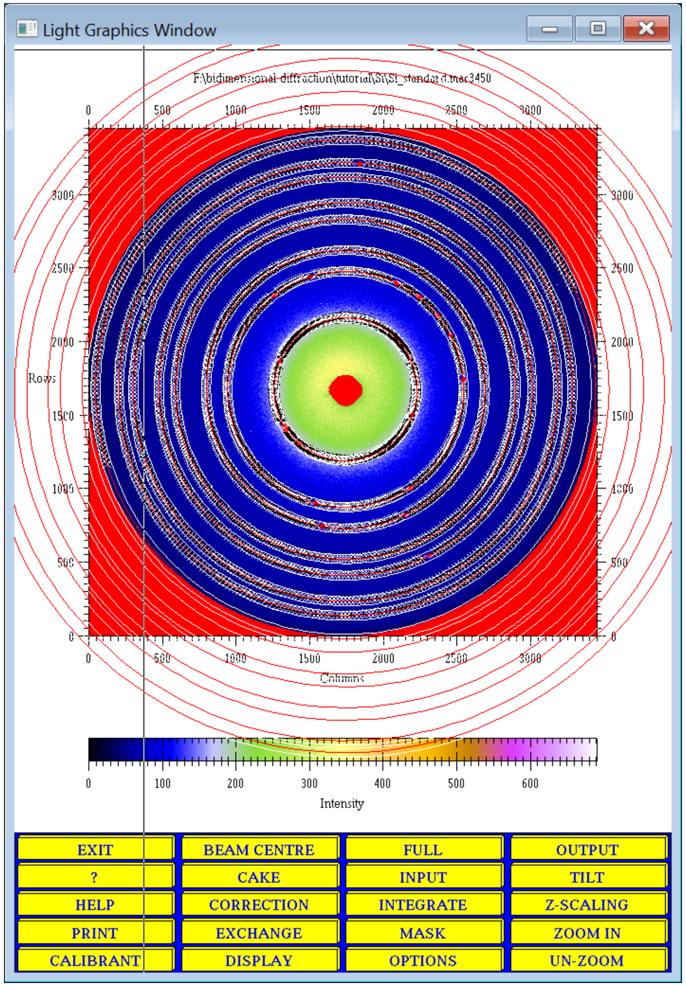

Need to check, cake it

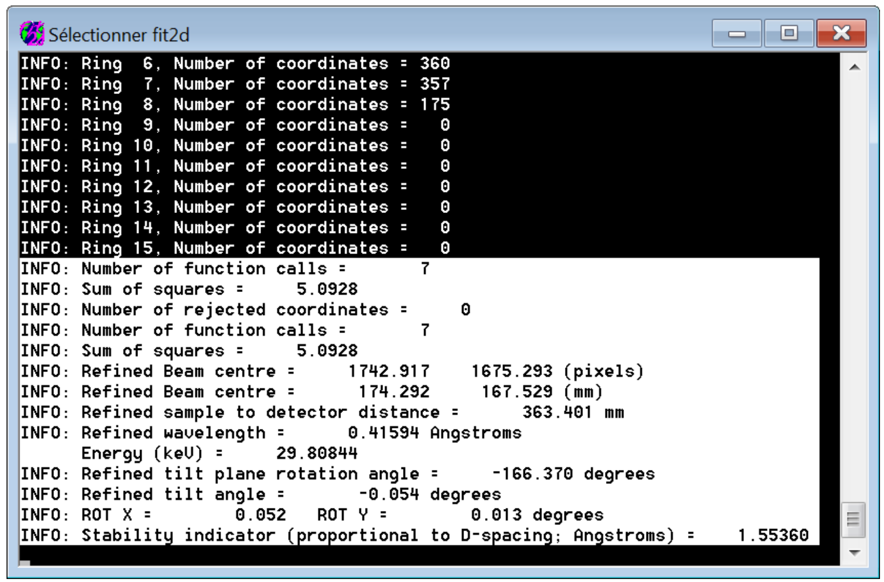

Cake

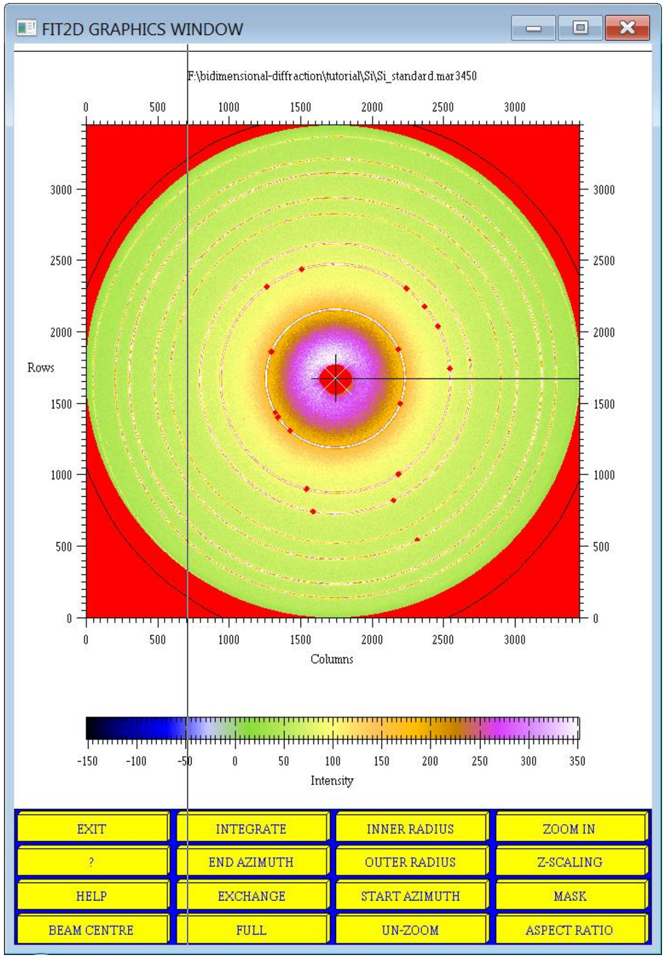

- We define an azimuthal start ,stop
- Inner radius outer radius
- Number of azimuthal bins
- Number of 2theta bins

- Intensity conservation
- Polarization correction
- polarization factor
- Geometrical correction for intensity

Azimuthal plot

- Azimuthal plot represent line → OK

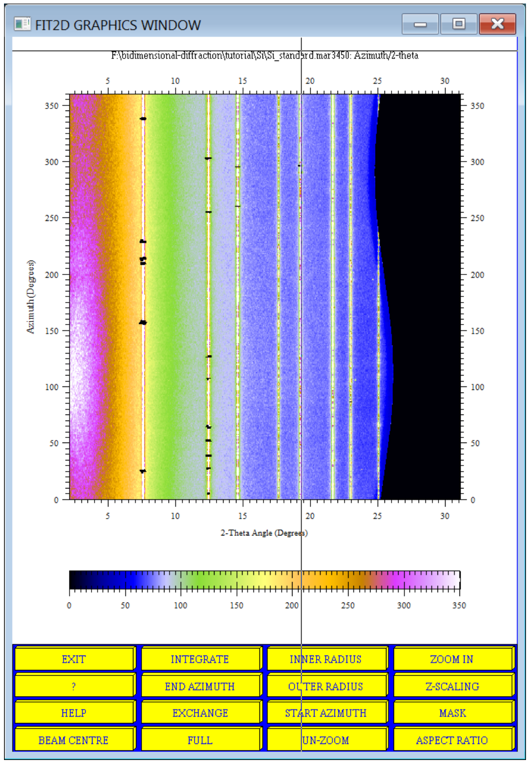

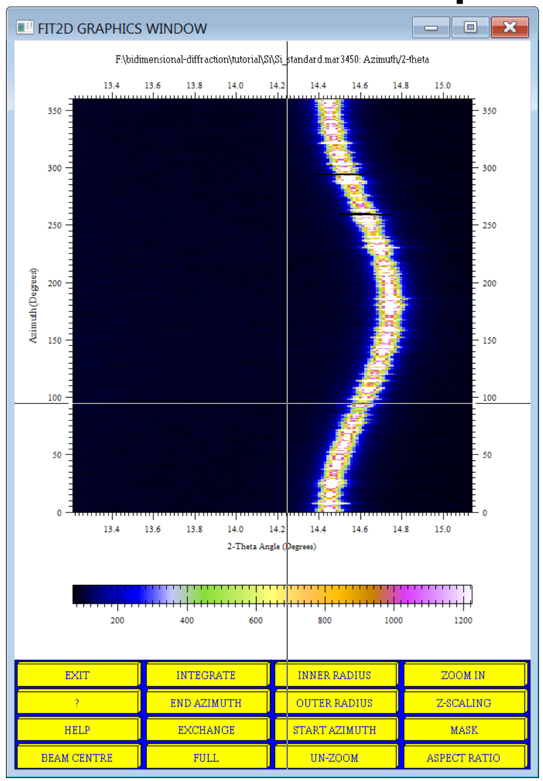

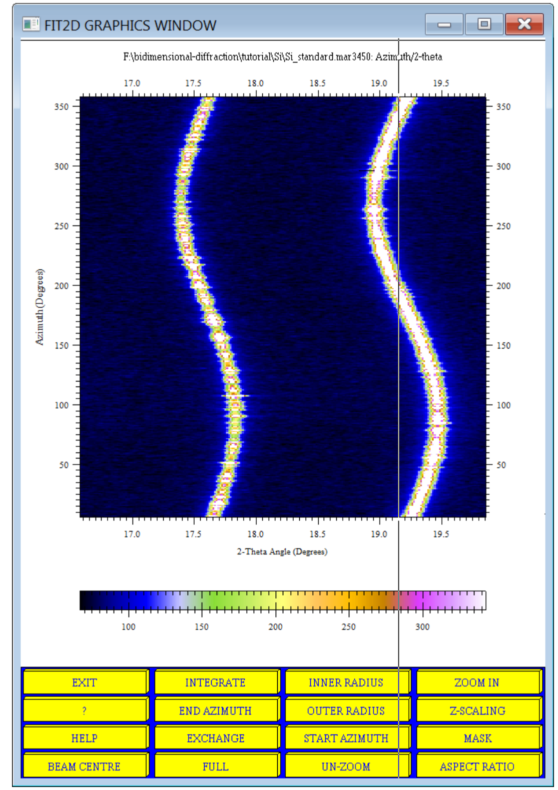

Wrong center

Wrong rot or tilt angle

Integral of azimuthal scan

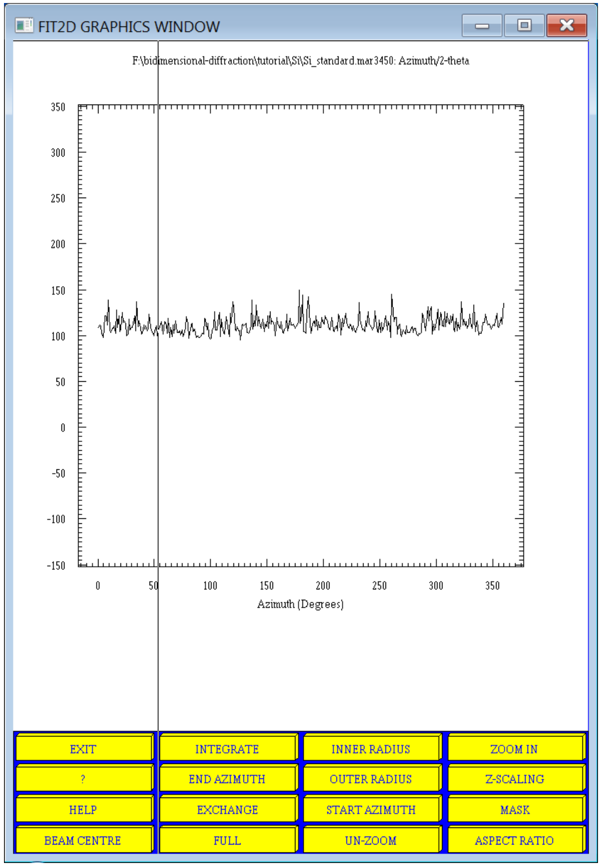

Good mask

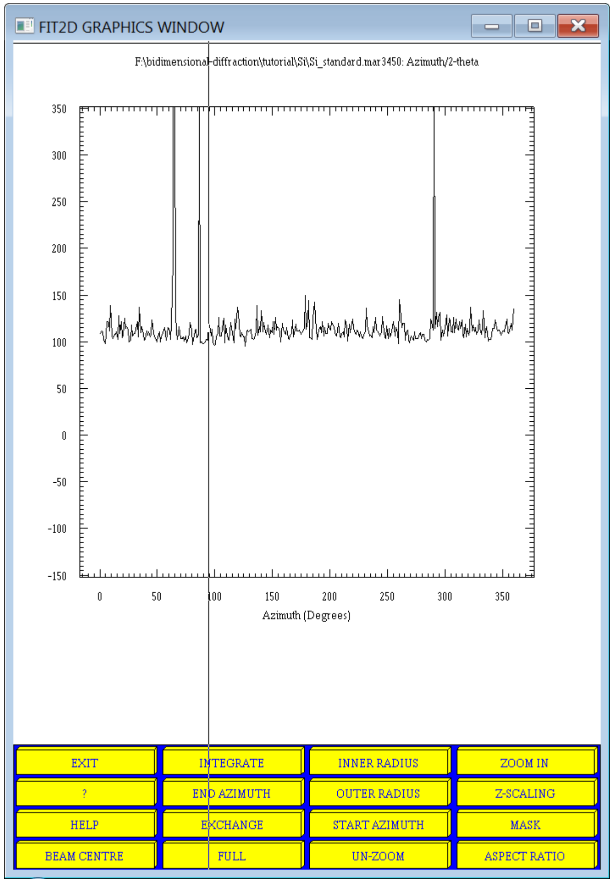

Few outliner

Sciences Chimiques de Rennes UMR CNRS 6226

Integration

- Possibility of save or fit peaks also iteratively with mfit

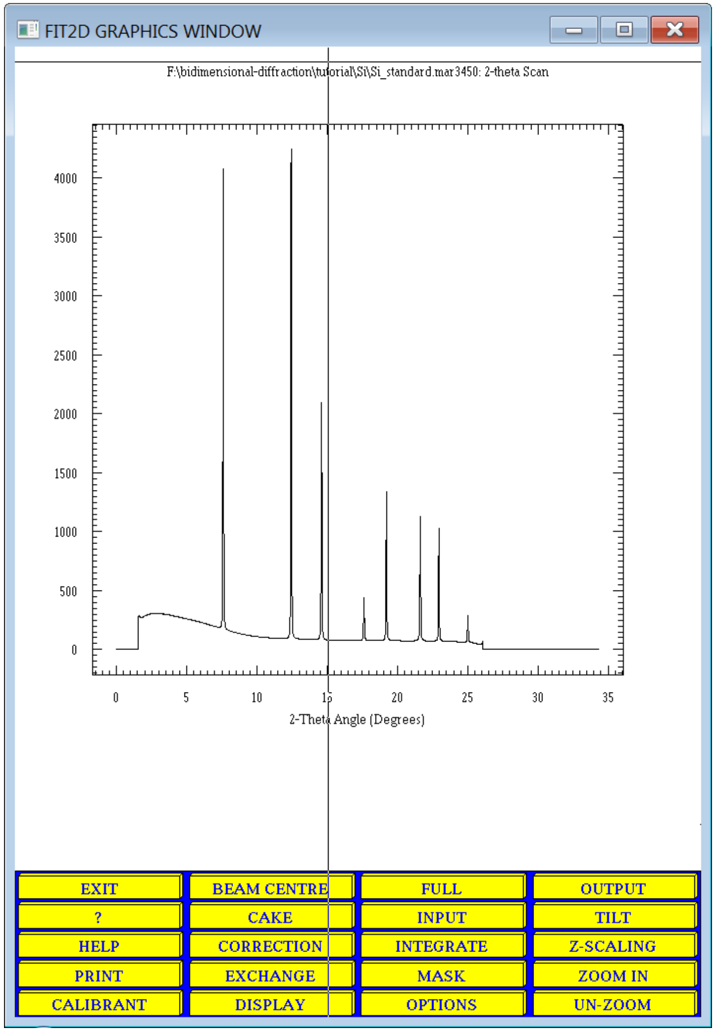

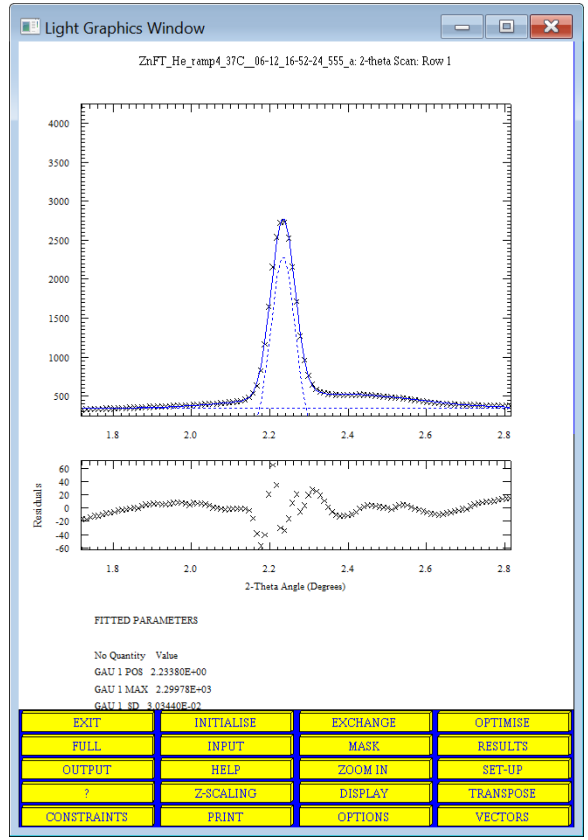

Macros

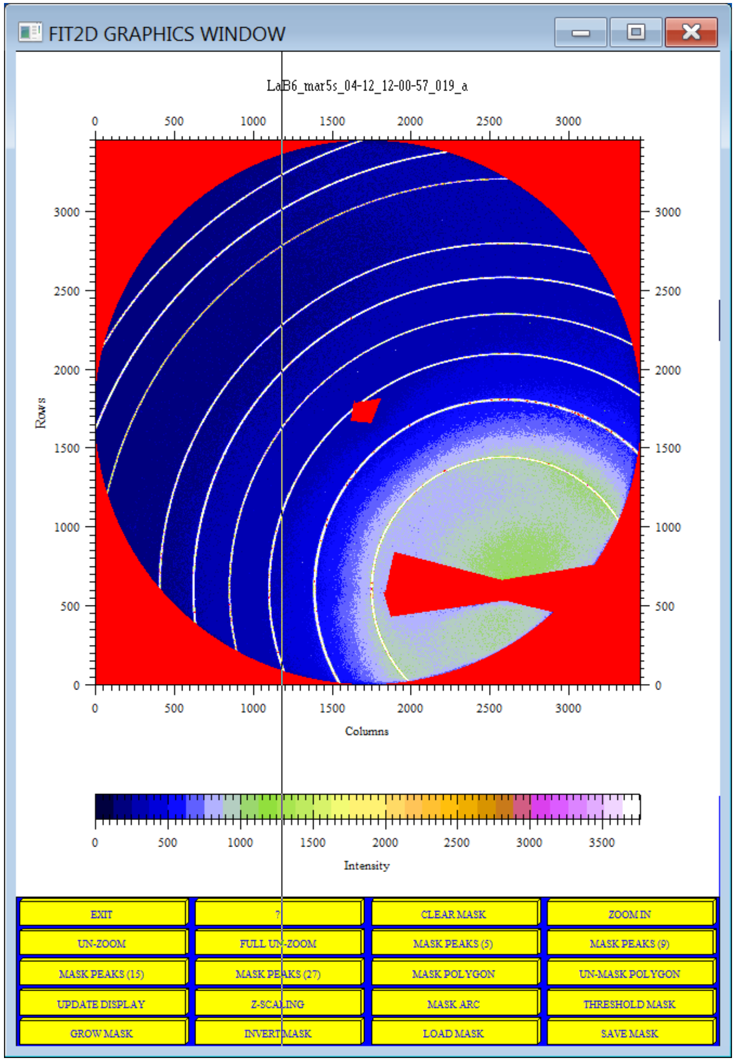

start with calibration

Exit

Macros/logfile   Create a macro Exit

Powder Diffraction

Input   (Open a file of the bach)

Integrate, output, exit

Macros/logfile   STOP macro Exit

Macro files

```
%!*\ This is a comment line
EXIT
ON-LINE CRYSTALLOGRAPHY
INPUT
F:I\ZnFT_72_2\ZnFT_He_r_555_a.edf
EXIT
POWDER DIFFRACTION (2-D)
INTEGRATE
O.K.
O.K.
OUTPUT
CHIPLOT
O.K.
EXCHANGE
EXIT
MACROS / LOG FILE
%!*\ END OF IO MACRO FILE
```

Change
input file>>>#IN
Output>>>#OUT

```
%!*\ This is a comment line
EXIT
ON-LINE CRYSTALLOGRAPHY
INPUT
#IN
EXIT
POWDER DIFFRACTION (2-D)
INTEGRATE
O.K.
O.K.
OUTPUT
CHIPLOT
O.K.
EXCHANGE
EXIT
MACROS / LOG FILE
%!*\ END OF IO MACRO FILE
```

Run sequence

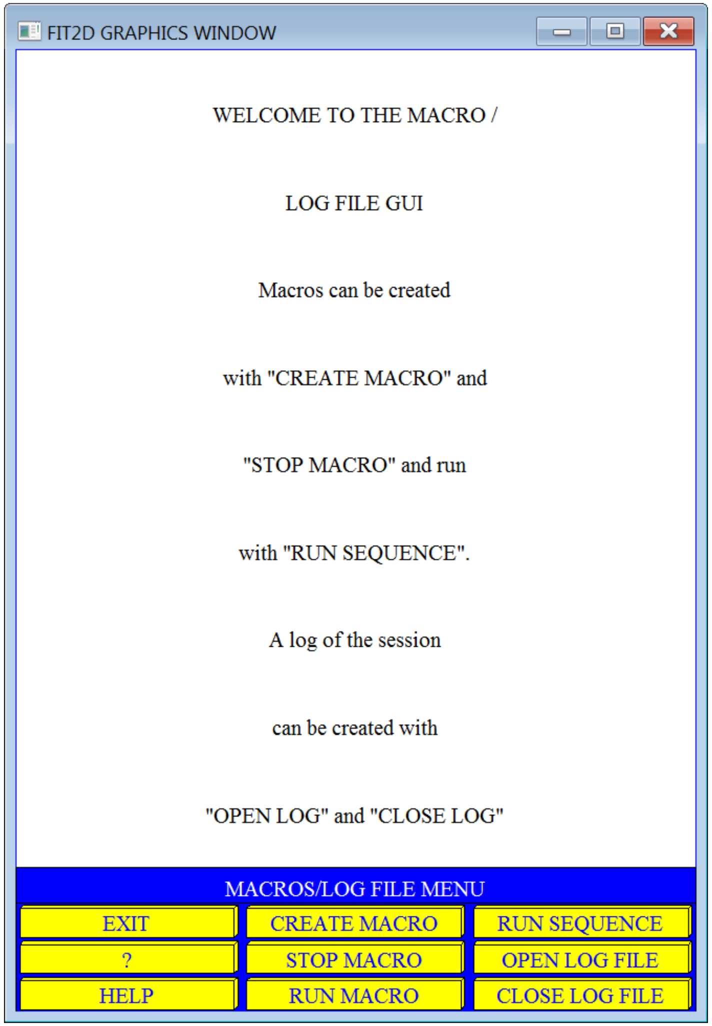

Run sequence
First file of the batch, last file, increment

And wait

Alternative option for non sequential name

- Write a file with all the instruction or generate it with sed and awk

```
%!*\ BEGINNING OF GUI MACRO FILE
%!*\
%!*\ This is a comment line
%!*\
EXIT
POWDER DIFFRACTION (2-D)
INPUT
F:\Data-SOLEIL-CRISTAL-20130419-dec13\Audebrand-MAR345\ZnFT_72_2\ZnFT_But_RT_06-12_19-43-12_619_a.edf
O.K.
INTEGRATE
O.K.
O.K.
OUTPUT
CHIPLOT
O.K.
INPUT
F:\Data-SOLEIL-CRISTAL-20130419-dec13\Audebrand-MAR345\ZnFT_72_2\ZnFT_He_ramp4_100C__06-12_18-11-53_587_a.edf
O.K.
INTEGRATE
O.K.
O.K.
OUTPUT
CHIPLOT
O.K.
INPUT
F:\Data-SOLEIL-CRISTAL-20130419-dec13\Audebrand-MAR345\ZnFT_72_2\ZnFT_He_ramp4_100C__06-12_18-14-12_588_a.edf
O.K.
INTEGRATE
O.K.
O.K.
OUTPUT
CHIPLOT
O.K.
INPUT
F:\Data-SOLEIL-CRISTAL-20130419-dec13\Audebrand-MAR345\ZnFT_72_2\ZnFT_He_ramp4_100C__06-12_18-16-38_589_a.edf
O.K.
INTEGRATE
O.K.
O.K.
OUTPUT
CHIPLOT
O.K.
INPUT
F:\Data-SOLEIL-CRISTAL-20130419-dec13\Audebrand-MAR345\ZnFT_72_2\ZnFT_He_ramp4_104C__06-12_18-18-59_590_a.edf
O.K.
INTEGRATE
O.K.
O.K.
OUTPUT
CHIPLOT
O.K.
INPUT
F:\Data-SOLEIL-CRISTAL-20130419-dec13\Audebrand-MAR345\ZnFT_72_2\ZnFT_He_ramp4_108C__06-12_18-21-19_591_a.edf
O.K.
INTEGRATE
O.K.
```

Further reading

- Powder DiffractionTheory and Practice
  Chapter 14 Two-dimensional Diffraction Using Area Detectors
  HINRICHSEN, DINNEBIER AND JANSEN
  (first part of presentation is mainly based on it)

- Two-dimensional_X-ray_Diffraction B. B. He

- Norby, P. (1997) Synchrotron Powder Diffraction using Imaging Plates: Crystal Structure Determination and Rietveld Refinement. J App Crys 30, 21-30.
- A P Hammersley, S O Svensson, and A Thompson, H Graafsma, ˚A Kvick, and J P Moy,“Calibration and correction of distortions in 2D detector systems”, Rev. Sci. Instr., (SRI-94), 66, 2729-2733 (1995)

- A P Hammersley, S O Svensson, M Hanfland, A N Fitch, and D Hausermann, “Two-Dimensional Detector Software: From Real Detector to Idealised Image or Two-ThetaScan”, High Pressure Research, 14, 235-248 1996